Biochimica et Biophysica Acta, 1024 (1990) 61–81
Elsevier

BBAMEM 74822

NMR, calorimetric, spin-label, and optical studies on a trifluoromethyl-substituted styryl molecular probe in dimyristoylphosphatidylcholine vesicles and multilamellar suspensions: a model for location of optical probes

B.P. Bammel [1,4], D.D. Hamilton [1], R.P. Haugland [2], H.P. Hopkins [1], J. Schuette [3], W. Szalecki [2] and J.C. Smith [1]

[1] *Department of Chemistry and Laboratory for Microbial and Biochemical Sciences, Georgia State University, Atlanta, GA,* [2] *Molecular Probes Inc., Eugene, OR,* [3] *Department of Chemistry, Emory University, Atlanta, GA and* [4] *Department of Chemistry, Boise State University, Boise, ID (U.S.A.)*

(Received 6 November 1989)

Key words: NMR, ^{19}F-; NMR, ^{13}C-; Calorimetry; Phase transition; Molecular probe; Fluorescence lifetime; Spin label; Phospholipid vesicle

NMR, calorimetric, and optical spectroscopic studies have been performed on a trifluoromethyl-substituted styryl molecular probe bound to vesicles and multilamellar suspensions formed from dimyristoylphosphatidylcholine (DMPC). In the fluorine NMR spectrum at 35 °C there are two partially resolved resonances, but these collapse to an apparently single resonance at temperatures above 60 °C. However, a line-shape analysis is not consistent with exchange between two sites on an NMR time scale, and the two resonances are assumed to be due to probe sites in the inner and outer leaflets of the vesicles. Two fluorescence lifetimes, each associated with one of these sites, characterize the decay curves for the molecular probe bound to DMPC vesicles. The shift reagent Eu(FOD)$_3$ and several nitroxide spin labels covalently bound to lipophilic structures strongly attenuate the lower frequency component of the fluorine NMR spectrum and also shift the other resonance to higher frequencies. The effect of two spin labels on the probe fluorine T2 relaxation time has been used to estimate the distance between the spin label unpaired electron and the trifluoromethyl group. The location of the spin label site in the membrane was determined from the effect of the unpaired electron on the lipid ^{13}C linewidths. A model for the location of the probe in the bilayer was developed from the above information and refined using molecular mechanics calculations on a probe-DMPC lipid complex. The long axis of the probe parallels the bilayer normal; the styryl-group portion of the optical chromophore is located slightly below the glycerol backbone, and the remainder of the chromophore extends well into the hydrophobic region of the bilayer. Therefore, the optical properties of the probe should not be significantly influenced by alterations of the membrane surface charge density. Parameters derived from DSC studies in the gel-to-lipid crystal phase transition of DMPC are extremely sensitive to the probe. Even at 0.0001 mol fraction of probe, the transition is substantially broadened, and the ΔH for the transition has increased, just as one predicts for the formation of a tight complex described above.

Introduction

Potential-sensitive molecular probes of the polyene class are of proven utility in diverse biological preparations ranging from model membrane systems to intact tissue and organ level studies. These probe applications have been described in reviews by Waggoner [1–3], Bashford and Smith [4], Bashford [5], Smith [6], and Cohen and Salzberg [7]. The applications of these indicators to the detection of the action potential in the

Abbreviations: CUP, cooperative unit parameter; DMPC, L-α-dimyristoyl-*sn*-glycero-3-phosphocholine; DMPG, L-α-dimyristoylphosphatidyl-DL-glycerol, sodium salt; DSC, differential scanning calorimetry; EDTA, ethylenediaminetetraacetic acid, disodium salt; Hepes, *N*-2-hydroxyethylpiperazine-*N'*-2-ethanesulfonic acid; NBD-Cl, 4-chloro-7-nitrobenzofuran.

Correspondence: J.C. Smith, Department of Chemistry and Laboratory for Microbial and Biochemical Sciences, Georgia State University, Atlanta, GA 30303-3053, U.S.A.

squid giant axon preparation [8,9] and to intercellular communication among small groups of cells such as the leech ganglion have been covered in a monograph edited by De Weer and Salzberg [10]. A multivolume series covering probe work on systems ranging from model membranes to organ level studies has been edited by Loew [11].

In energy transducing preparations such as mitochondria, submitochondrial particles, and in sarcoplasmic reticulum vesicles, uncertainties regarding the nature of the potential(s) to which polyene and other types of probes are sensitive have remained a persistent problem in the interpretation of results obtained with these dyes. Among the possibilities are surface charge density alterations, intramembrane charge gradients [12], membrane Bohr effects [13], and transmembrane potentials. The membrane surface charge density and changes in it play an important role in the energy transduction mechanism proposed by Malpress [14] in which discrete surface charge formation is linked to electron transport. Kell's mechanism [15] invokes properties of the unstirred layer adjacent to the membrane, which are in part controlled by the surface potential according to the Gouy-Chapman theory of the diffuse double layer. The collisional model of energy transfer from the electron transport chain to the mitochondrial ATPase proposed by Slater et al. [16] would also likely be sensitive to membrane surface charge.

Based on the lack of an effect of NBD-Cl inhibition of ATPase activity in submitochondrial particles on the kinetics of the ATP-dependent ANS fluorescence signal, Ferguson [17] has proposed that this indicator may be sensing local events, presumably charge separation, at the level of the ATPase and thus may not be a reliable indicator of delocalized potential in these latter preparations. Also, ANS appears to be sensitive to the surface potential in sarcoplasmic reticulum preparations in low ionic strength media [18,19]. The uncertainty in the relative sensitivity of ANS and related *N*-arylnaphthalene probes to local vs. delocalized potentials and to surface potentials in the preceding preparations has in part led to the development of a large number of potential-sensitive molecular probes, primarily of the polyene class, for which many applications have been previously described. Kinally et al. [20], however, have proposed that a number of polyene-type dyes of the carbocyanine class are primarily sensitive to surface charge rather than to transmembrane potential in mitochondria; but Laris et al. [21] have obtained values of the membrane potential with those probes that are in agreement with values obtained by independent techniques based on the distribution of permeant ions across the mitochondrial membrane.

The relative sensitivity of these and related probes to surface potentials vs. transmembrane potentials is particularly crucial during massive ion translocation such as Ca^{2+} uptake or release in mitochondria or sarcoplasmic reticulum vesicles. Beeler et al. [22] and Russell et al. [23] have, for example, noted that the probe WW781 is unresponsive to transmembrane diffusion potentials and appears to sense only surface phenomena in the latter preparation. Other probes, such as oxonol VI and nile blue A, have varying sensitivities to surface charge density changes relative to transmembrane potentials; furthermore, the probe response to the latter two charge gradients could not be readily distinguished since the optical signals from the two sources were qualitatively identical. The preceding problems and discrepancies are at least in part dependent on the location of the probes in the membrane bilayer.

Probes of the styryl class, such as RH 160, have been shown by Ehrenberg et al. [24] to respond to charge separation in the bacteriorhodopsin photocycle on a microsecond time scale. Indicators of this type, primarily RH 414, have also been used in investigations of the rat somatosensory cortex [25] and visual cortex of the monkey [26]. The location of these probes in the bilayer is of critical importance since they respond to charge separation by an electrochromic or charge-shift mechanism and can sense only that portion of the potential gradient that develops across the probe's molecular dimension.

This paper contains results derived from a combination of techniques based on magnetic resonance, optical spectroscopy, and calorimetry that have been used to estimate the location of a trifluoromethyl label placed on a styryl-type molecular probe in well defined model membrane preparations consisting of small unilamellar dimyristoylphosphatidylcholine (DMPC) vesicles or multilamellar DMPC suspensions.

Conclusions derived from these experiments have been compared to energy minimization calculations based on molecular mechanics. These calculations were performed on the fluorinated probe in the presence of two DMPC lipids in a monolayer configuration; but only one location of the probe gave a well-defined minimum.

Materials and Methods

L-α-Dimyristoylphosphatidylcholine was purchased from Avanti Polar Lipids, Birmingham, AL. The fluorinated molecular probe was synthesized by Molecular Probes, Inc., and the structure (Fig. 1) verified by elemental analysis, mass spectroscopy, and ^{1}H- and ^{19}F-NMR analyses, Hepes (*N*-2-hydroxyethylpiperazine-*N'*-2-ethanesulfonic acid) was supplied by the Sigma Chemical Co., and all other reagents, which were of ACS reagent grade or better, were obtained from the Fisher Scientific Co.

Sample preparation and handling procedures

DMPC vesicles were prepared using a modified form of the procedure developed by Suurkuusk et al. [27], previously described [28]. Lipid was suspended in 160 mM KCl, 10 mM Na-Hepes (pH 7.4), and 0.1 mM EDTA (Hepes buffer), and the suspension was sonicated at 35°C under nitrogen with a half-inch probe device for 60 min at a 30 percent duty cycle. Centrifugation at 130000 × *g* was used to separate the resulting vesicles from probe and other debris.Vesicle lipid concentrations were obtained using a colorimetric phosphate assay developed by Heinonen and Lahti [29].

The vesicle preparations were monitored by electron microscopy using a negative staining procedure based on uranyl acetate [28] and found to have diameters in the 300–350 Å range. The vesicle suspensions were stored in an oven maintained at 35°C and were stable for about four days under these conditions.

The nitroxide-type lipophilic spin labels (Fig. 1) used in our investigations were supplied by Molecular Probes, Inc. Two protocols were used to introduce these spin labels into the DMPC vesicles: (1) the label was added to the vesicles suspended at 35°C and was continually stirred overnight; (2) the spin label and lipid were dissolved in chloroform in a round bottom flask and the solvent removed by swirling the flask to induce evaporation. Residual solvent was then removed by maintaining the flask and contents under reduced pressure for 24 h. Vesicles were then formed from this mixture according to the previously described protocol. The uniformity of the spin label distribution in the vesicle bilayer was ascertained by monitoring the EPR spectrum from the resulting DMPC vesicle preparation.

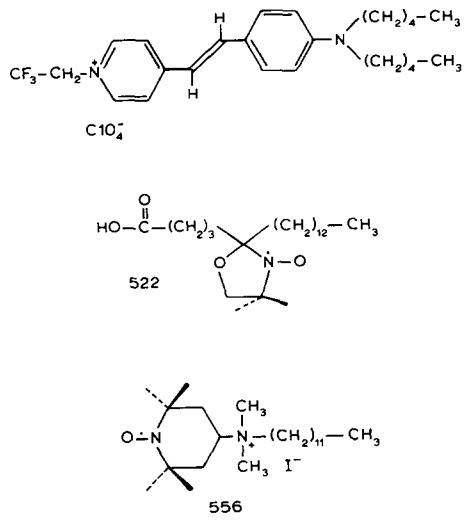

Fig. 1. The structure of the fluorine labeled molecular probe, 4(4-dipentylamino-*trans*-β-styryl)-1-(2,2,2-trifluoroethyl)pyridinium perchlorate, and the two spin labels: No. 522, 2-(3-carboxypropyl)-4,4-dimethyl-2-tridecyl-3-oxazolidinyloxide; and No. 556, dodecyldimethyl[(2,2,6,6-tetramethyl-1-piperidyloxide)-4-yl]ammonium iodide.

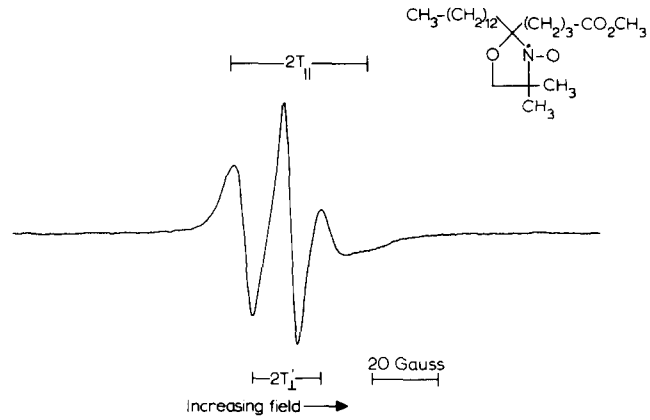

Fig. 2. The EPR spectrum of DMPC vesicles with added spin label No. 523, 4,4-dimethyl-2-[3-(methoxycarbonyl)propyl]-2-tridecyloxazolidin-3-yl oxide, the structure of which is shown in the inset. The spin label was present at 5 mol% and the vesicles were suspended at 10 mM concentration in aqueous solution of 160 mM KCl, 10 mM Na-Hepes (pH 7.5), and 0.1 mM EDTA and at 23°C. The spectrum was obtained using an IBM Instruments/Brooker ER200D spectrometer operating at 9.8 GHz.

The presence of shoulders on the three typical resonances from the first derivative spectrum was taken to indicate nonuniformity in the spin label distribution. The procedure based on the use of the chloroform solvent consistently resulted in symmetrical EPR lines with no detectable side resonances or shoulders. An IBM/Brooker ER200D X-band spectrometer was used to obtain the EPR spectra. A typical spectrum, taken at 23°C, from Molecular Probe spin label No. 523 is illustrated in Fig. 2. The reduction in the lines to lower and higher field of the central resonance is characteristic of restricted motion expected for the vesicle-bound spin label. This spectrum is somewhat similar to that observed from the same spin label in multilamellar egg PC dispersions by Gordon et al. [30], but the splitting of the resonances in the spectrum from the DMPC vesicles is not as pronounced as that from the egg PC dispersions, apparently due to the enhanced averaging of the dipolar itneraction terms in the spin hamiltonian by the global tumbling of the vesicles. In particular, the splitting of the line located to lower field of the central resonance observed by Gordon et al. [30] in egg PC dispersions is not detectable in the illustrated spectrum from the same spin label bound to unilamellar DMPC vesicles.

Since the static hyperfine interaction tensor components ($T_{xx} = T_{yy} = 6.1$ G; $T_{zz} = 32.4$ G) have been determined by doping the spin label into a crystal lattice [31], it is possible to obtain an estimate of the order parameter characterizing the motion of the spin label-DMPC system from the parallel and perpendicular components of the hyperfine tensor obtained from the spectrum (Fig. 2). In the tensor component evaluation, the X axis is taken as a parallel to the N-O bond, and

the Z axis is directed along the nitrogen $2p_z\pi$ orbital and $2T'_\perp = 2T_\perp - 1.6$ G [29]. Values obtained for the parallel and perpendicular components are: $T_\parallel = 21$ G and $T_\perp = 11.6$ G. Order parameters are evaluated from $T_\parallel$ and $T_\perp$ values using the relationships [30]

$$S(T_\parallel) = \frac{3(T_\parallel - T_{xx})}{2(T_{zz} - T_{xx})} - 1 = 0.36 \quad (1)$$

$$S(T_\perp) = \frac{3[(T_{zz} + T_{xx}) - 2T_\perp]}{2(T_{zz} - T_{xx})} - 1 = 0.38 \quad (2)$$

These values have not been corrected for the polarity difference in the spin label sites in the crystal and DMPC vesicle bilayer. As discussed by Gordon et al. [30], however, a correction to the apparent order parameter for the polarity difference may be obtained by dividing the hyperfine tensor components by the isotropic hyperfine coupling constant because the latter quantity is sensitive to the polarity of the environment of the spin label. These corrections, when applied to either $S(T_\parallel)$ or $S(T_\perp)$ yield

$$S = \frac{T_\parallel - T_\perp}{T_{zz} - T_{xx}} \cdot \frac{(a_N)}{(a'_N)} = 0.36 \quad (3)$$

where $a_N = (1/3)(T_{zz} + 2T_{xx})$ and $a'_N = (1/3)(T_\parallel + 2T_\perp)$ are the coupling constants describing the hyperfine interactions in the spin label located in the host crystal and DMPC vesicle bilayer, respectively. Hubbel and McConnel [32] derived Eqn. 3 based upon the assumption that T_{xx} and T_{zz} are affected in the same manner by the crystal and membrane polarity difference.

The value of S, $S(T_\parallel)$ and $S(T_\perp)$ obtained from the DMPC vesicle preparation are significantly and consistently lower than the corresponding values of 0.60, 0.59 and, 0.61 obtained by Gordon et al. [29] in egg PC dispersions. The global tumbling motion of the vesicles, which is greatly reduced in multilamellar dispersions, is expected to cause these parameters to be significantly smaller.

NMR spectroscopy

A Varian VXR400 spectrometer was used to obtain ^{19}F spectra at 376 MHz in a 5 mm H/F probe and ^{13}C spectra at 100.6 MHz with a 10 mm broad band probe. Spectra involving the DMPC vesicles were routinely obtained at 25 °C with proton decoupling. Fluorine spin-lattice, T1, and spin-spin, T2, relaxation times were measured using the inversion recovery method and the CPMG pulse sequence, respectively. The frequency scales for all fluorine NMR spectra are relative to trifluoroacetic acid that was employed as an external reference, ^{13}C chemical shift scales have been developed relative to the DMPC terminal methyl resonance which served as an internal reference as described in the Results.

Fluorescence spectroscopy

The fluorescence emission or excitation spectra of the molecular probe in glycerol, in Hepes buffer, or bound to DMPC vesicles were obtained using a Hitachi-Perkin Elmer MPF44 fluorometer interfaced to an IBMPC/AT computer via software and hardware supplied by On-Line Instrument Systems, Inc. Polarized emission and excitation spectra were obtained using Polaroid film type polarizers mounted in the exciting and emitted light beams. Fluorescence lifetime measurements were performed using a Photochemical Research Associates photon counting system equipped with a hydrogen arc lamp and a cooled photomultiplier housing; this device has a lifetime resolution of approx. 0.5 ns.

Calorimetry

Simply adding the probe to the suspension or to the lipid before vortexing with buffer provided samples with non-reproducible DSC scans; however, these problems were alleviated when suspensions were prepared from thin films of the lipid and probe in methanol solutions. A stock solution of the probe was prepared by dissolving a known weight into a known volume of methanol. This solution (extinction coefficient of 74 800 $M^{-1} \cdot cm^{-1}$ at the absorbance maximum of 529.3 nm) was used to add known quantities of probe to methanol solutions containing DMPC. These solutions, prepared in glass vials, were evaporated to thin films by passing nitrogen over the surface while swirling; these films were then subjected to vacuum for 10 to 12 h to remove any residual methanol. A known volume of 10 mM Na-Hepes (pH 7.2), 160 mM KCl, and 0.1 mM EDTA was added to the vial. Vortexing for 5–0 min produced multilamellar suspensions which were stable for several hours if the solution was first heated to 40 °C. These solutions were immediately placed in the DSC and scanned as soon as possible. After all scans were completed, six to eight aliquots of the freshly vortexed suspensions were analyzed for phosphate [33] with a standard deviation always less than 3 percent. The resulting phosphate concentrations were used to calculate the moles of DMPC in the calorimetric cell.

The excess heat capacity of the main gel-to-liquid crystal DMPC phase transition relative to the buffer was measured as a function of temperature using a Microcal MC2 scanning differential calorimeter (DSC). A scanning rate of 1.8 C°/h was used when the probe mol percent was equal to or less than 0.01, in order to avoid distorting the very sharp heat capacity profiles characterizing this system. When the probe was present at mol percents greater than 0.01, the profiles were sufficiently broad that identical curves were obtained

with either 1.8 or 7.2 C°/h rates. Because of the extremely pure lipid use in these studies, the gel-to-lipid crystal phase transition was only 0.05 C° wide at the half-height; the 1.8 C°/h rate and filtering of the temperature signal were necessary to produce scans with reproducible areas and peak heights.

The enthalpy, ΔH_{Cal}, characterizing the DMPC gel-to-liquid crystal phase transition was obtained from the area under the excess heat capacity profile and was evaluated by the software package provided by Microcal, Inc. The corresponding van't Hoff enthalpy was obtained from

$$\Delta H_{vH} = 4RT_m^2 \Delta C_p(\max)/\Delta H_{Cal} \quad (4)$$

which assumes that the gel-to-liquid crystal transition can be described as a two-state process [34–36]; $\Delta C_p(\max)$ and T_m are the excess heat capacity and corresponding temperature at the maximum of the heat capacity vs. temperature profile. The Microcal software package evaluated T_m and $\Delta C_p(\max)$ and performed the indicated calculations in Eqn. 4 to obtain ΔH_{vH}. In the absence of cooperativity, the ratio $\Delta H_{vH}/\Delta H_{Cal}$ should be unity, but for highly cooperative processes, such as the DMPC main phase transition, this ratio may significantly exceed unity. This ratio is defined as the cooperative unit parameter (CUP). In the case of the multilamellar DMPC gel-to-liquid crystal phase transition, however, the CUP is not necessarily a direct measure of the number of lipids melting as a unit, i.e., the cluster size, but is merely a parameter that provides a measure of cooperativity [37].

Results and Data analyses

NMR spectroscopy

The fluorine NMR spectrum of the molecular probe dissolved in CD_3OD is illustrated in Fig. 3 and consists of the expected triplet. Protons on the methylene group located between the trifluoromethyl group and the quaternary nitrogen moiety in the ring system are acidic due to the electron withdrawing properties of those groups, and the exchange of the methylene protons with deuterium from the solvent produced, over time, two groups of resonances consisting of a doublet and a singlet corresponding to the -CHD- and $-CD_2-$ probe species being observed, since the fluorine-deuterium coupling interaction is weak. The inset in Fig. 3 shows the spectrum of a solution several weeks old with proton decoupling so that the fluorine-proton splittings are removed. This exchange process was complete after several weeks, but caused no problems in the work with

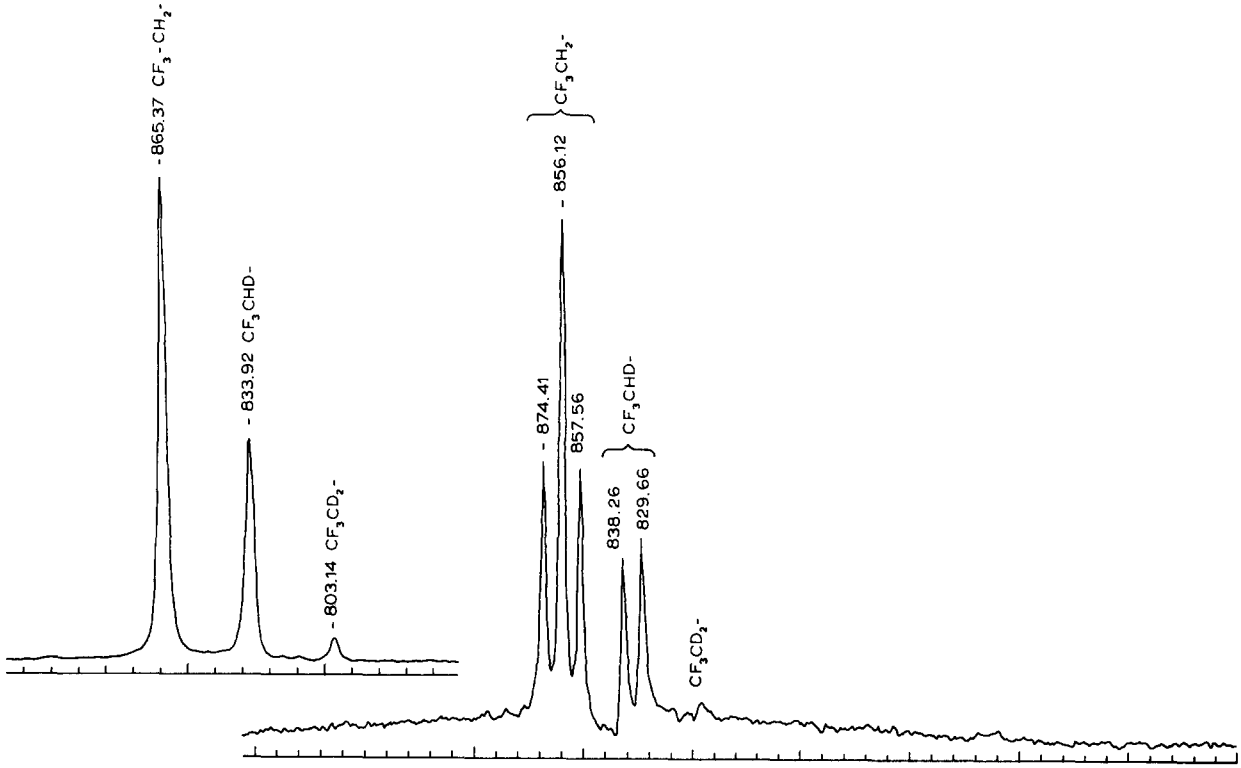

Fig. 3. The fluorine NMR spectrum at 20 °C for the probe, whose structure is shown in Fig. 1, dissolved in CD_3OD at 2.6 mM. Eight transients were averaged to obtain this spectrum using a Varian VXR 400 spectrometer operating at 376 MHz with a broadening factor of 1 Hz. The three groups of resonances are due to three probe species, generated by the exchange of acidic methylene protons with deuterium from the solvent. The fluorine spectrum shown in the inset was obtained with proton decoupling and the average of 64 transients. The indicated frequencies were evaluated relative to an external reference of trifluoroacetic acid 5 mM in CD_3OD.

TABLE I

The effect of the shift reagent Eu(FOD)$_3$ on the fluorine spin-lattice and spin-spin relaxation times of the molecular probe whose structure is shown in Fig. 1

The molecular probe was dissolved in CD_3OD at 2.6 mM. The spectra from which the relaxation times were derived were obtained at 376 MHz with proton decoupling at 20 °C from an average of eight transients. The inversion recovery method and the CPMG pulse sequence were used to measure the T1 and T2 values, respectively. Peaks 1, 2 and 3 correspond to the CF_3-CH_2-, CF_3-CHD-, and CF_3-CD_2- species, respectively, that arise from the exchange of the acidic methylene protons with deuterium from the solvent; see Results for details. Thresholds in the Eu(FOD)$_3$ shift reagent concentration of 0.5 and 1 mM were necessary to generate significant reductions in the fluorine T1 and T2 relaxation time values, respectively. The error in duplicate measurements of the relaxation times was 3 percent.

Eu(FOD)$_3$ concn. (mM)	T1 (s)			T2 (s)		
	Peak 1	Peak 2	Peak 3	Peak 1	Peak 2	Peak 3
Control	0.613	0.632	0.656	0.393	0.463	0.453
0.05	0.613	0.632	0.656	0.386	0.449	0.588
0.5	0.538	0.559	0.602	0.386	0.449	0.580
1.0	0.505	0.522	0.572	0.321	0.363	0.366

the DMPC vesicles in aqueous solution with D_2O present at ten percent (v/v) to provide a lock signal. Table I contains a summary of the fluorine relaxation times obtained from solutions of the probe in CD_3OD. The T1 and T2 values as well as the effect of the shift reagent Eu(FOD)$_3$ on the relaxation rates associated with those two parameters are similar.

When bound to DMPC unilamellar vesicles, the fluorine NMR spectrum of the probe is sustantially broadened and undergoes a shift to lower frequency (downfield shift). Two partially resolved resonances, the maxima of which are separated by about 50 Hz were consistently observed in the fluorine NMR spectra of the probe bound to these vesicles (Fig. 4(A)). The fluorine NMR data were routinely obtained with proton decoupling, but the line widths were the same with or without decoupling, apparently due to the broadening caused by the slow motion of the vesicles. In experiments in which the spectral window was sufficiently large to encompass resonance frequencies associated with both the free probe and that bound to the DMPC vesicles, no signal associated with the free dye could be detected; thus, by this criterion, virtually all of the probe is bound to the vesicles at the lipid-to-dye mol ratios used in these investigations.

The fluorine NMR spectrum of the DMPC vesicle-bound molecular probe was a function of temperature as illustrated in Fig. 5(A). Increasing the temperature caused the separation between the two partially resolved resonances observed at 35 °C to monotonically decrease, until at 75 °C essentially a single resonance was observed. The frequencies at which the maxima in the unreferenced spectra were observed were also shifted systematically to higher values as the temperature was increased; the frequencies of the maxima associated with the spectra obtained at 35 and 75 °C differed by approximately 300 Hz. Since a similar temperature-dependent shift was observed in the resonance frequency of trifluoroacetic acid that was employed as an external reference, the temperature dependence of the probe ^{19}F resonance frequency is effectively removed in the data shown in Fig. 5(A). The presence of two resonances in the fluorine spectra of the DMPC-associated probe and the tendancy of these resonances to apparently collapse to a single line suggest that the probe occupies two different classes of sites in the vesicle bilayer and that these sites may undergo exchange on the NMR time

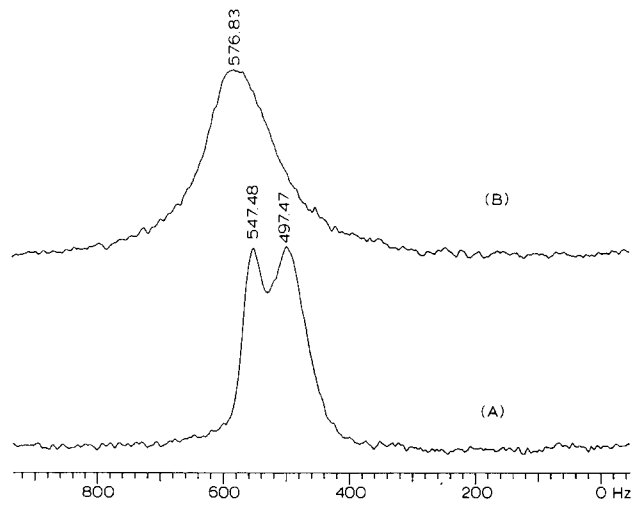

Fig. 4. (A) The ^{19}F-NMR spectrum of the fluorinated probe bound to DMPC vesicles suspended at 10 mM concentration in Hepes buffer and with a probe-to-lipid mol% of 1.7. The spectrum was obtained using a Varian VXR 400 spectrometer operating at 376 MHz with proton decoupling; 2048 transients were averaged to obtain the spectrum. The line broadening factor was 5 Hz and the sample temperature was 35 °C. The two partially resolved resonances separated by 50 Hz were consistently observed when the fluorinated probe was bound to these vesicles. (B) Spectrum with the presence of 5 mol% of spin label 522 (Fig. 1) in the sample described in part (A). The lower frequency resonance is essentially eliminated by the spin label and the remaining resonance is shifted to higher frequency. The frequency scales for these two spectra were derived from the fluorine resonance of trifluoroacetic acid that was employed as an external reference and was present at 5 mM in the same aqueous medium as used in all NMR work employing DMPC vesicles.

scale. Accordingly, the probe spectra shown in Fig. 5(A) were analyzed using the general line-shape function for two sites [38]:

$$\text{Ampl}(\omega) = (C[1+(\tau/2)(P_A/T2_B + P_B/T2_B)]P + QR)/(P^2 + R^2) \quad (5)$$

where Ampl is the signal amplitude, C is a scaling factor, and

$$P = P_A/T2_A + P_B/T2_B + (\tau/2)[1/T2_AT2_B - ((\omega - (\omega_A + \omega_B)/2)^2) + (1/4)(\omega_A - \omega_B)]$$

$$R = (\omega - (\omega_A + \omega_B)/2)[1 + (\tau/2)(1/T2_A + 1/T2_B)] + (\tau/4)(\omega_A - \omega_B)(1/T2_A - 1/T2_B) - (1/2)(P_A - P_B)(\omega_A - \omega_B)$$

and

$$Q = (\tau/2)[(\omega - (\omega_A + \omega_B)/2) + (1/2)(\omega_A - \omega_B)(P_A - P_B)]$$

The quantity τ is the mean lifetime associated with states A and B and is defined by

$$2/\tau = 1/\tau_A + 1/\tau_B$$

This analysis does not include coupling between the sites. The data analysis was performed on a UNIVAC 90/80 computer using a nonlinear regression routine developed by Johnson and Schuster [39]. In this analysis, the two spin-spin relaxation times (T2) were obtained with the CPMG pulse sequence. Typical T2 values from several experiments are collected in Table II. The experimentally determined T2 values were usually held constant in the exchange analysis procedure because it was found that these parameters and the mean lifetime τ were highly correlated. The fractional population associated with one of the two observed resonances, P_A, was allowed to vary and the second population value obtained from the normalization condition. The frequencies, ω_A and ω_B, associated with the two maxima observed in the spectra were also allowed to vary in this analysis. The data could be well described by this analysis as illustrated in Fig. 5(B): the actual NMR data obtained at 35°C are shown as triangles and the solid line is a theoretical curve. Only one half of the total number of points used in the analysis are plotted in the figure. The population parameters returned by the regression routine indicate that about 40 percent of the population, P_A, is associated with the higher frequency resonance, ω_A, and 60 percent with the remaining component. Initially we found that the spectrum obtained at 35°C could be fitted by the two-site exchange function using millisecond values for the lifetime. Values of this order of magnitude, however, could not be used to successfully reproduce the higher temperature spectra, which tended to approach a single Lorentzian line (Fig. 5(A)). At the higher temperature the analysis became insensitive to the value of the mean lifetime, provided that it was in the 10^4 to 10^5 s range. Typical values returned by the nonlinear regression routine are included in the caption to Fig. 5(B). The preceding results suggest that the two sites are approximately equally populated but are not undergoing exchange on the NMR time scale. Coalescence of the two resonances at the higher temperatures is probably due to a different temperature dependence for each fluorine chemical shift parameter, which is known to be highly temperature dependent.

The spectrum obtained at 35°C could be equally well described by two overlapping Lorentzian line-shape functions (Fig. 5(C)). The double Lorentzian analyses were performed using the nonlinear regression of Johnson and Schuster [39] or using an in-house, FORTRAN-based fitting routine running on an IBMPC/AT computer. The latter result is also consistent with the lack of an exchange process connecting the two apparent classes of sites occupied by the probe, since such a process is not included in the double Lorentzian analysis procedure.

The effects of a number of paramagnetic perturbants in the form of spin labels or shift reagents on the probe fluorine NMR spectrum were investigated in order to obtain information on the location of the probe in the DMPC bilayer. The addition of the spin labels (Fig. 1) and the shift reagent $Eu(FOD)_3$ either strongly at-

TABLE II

Summary of the correlation times, τ_c, fluorescence lifetimes, τ_F, the fluorine spin-spin relaxation times, T2, and the spin label to trifluoromethyl group distances, r, associated with the molecular probe illustrated in Fig. 1 bound to DMPC vesicles

The fluorine spin-spin relaxation times were measured using the CPMG pulse sequence under the experimental conditions described in the caption to Fig. 4. The measurement of the fluorescence lifetime and the calculation of the correlation time using the Perrin equation are described in Results and Data Analyses, as is the evaluation of the distance r from the spin label site to the probe trifluoromethyl group by means of Eqn. 6. All T2 values contained in this table were obtained from the same DMPC vesicle preparation. The structures of the spin labels identified by numbers in this table are provided in Fig. 1.

Spin label No.	τ_c (ns)	τ_F (ns)	T2 (control, ms)	T2 (control + spin label, ms)	r (Å)
522	2.17	0.7	23.5	3.6	9.4
522	9.94	3.2	23.5	3.6	12.2
556	2.17	0.7	23.5	7.7	11.1
556	9.94	3.2	23.5	7.7	14.3

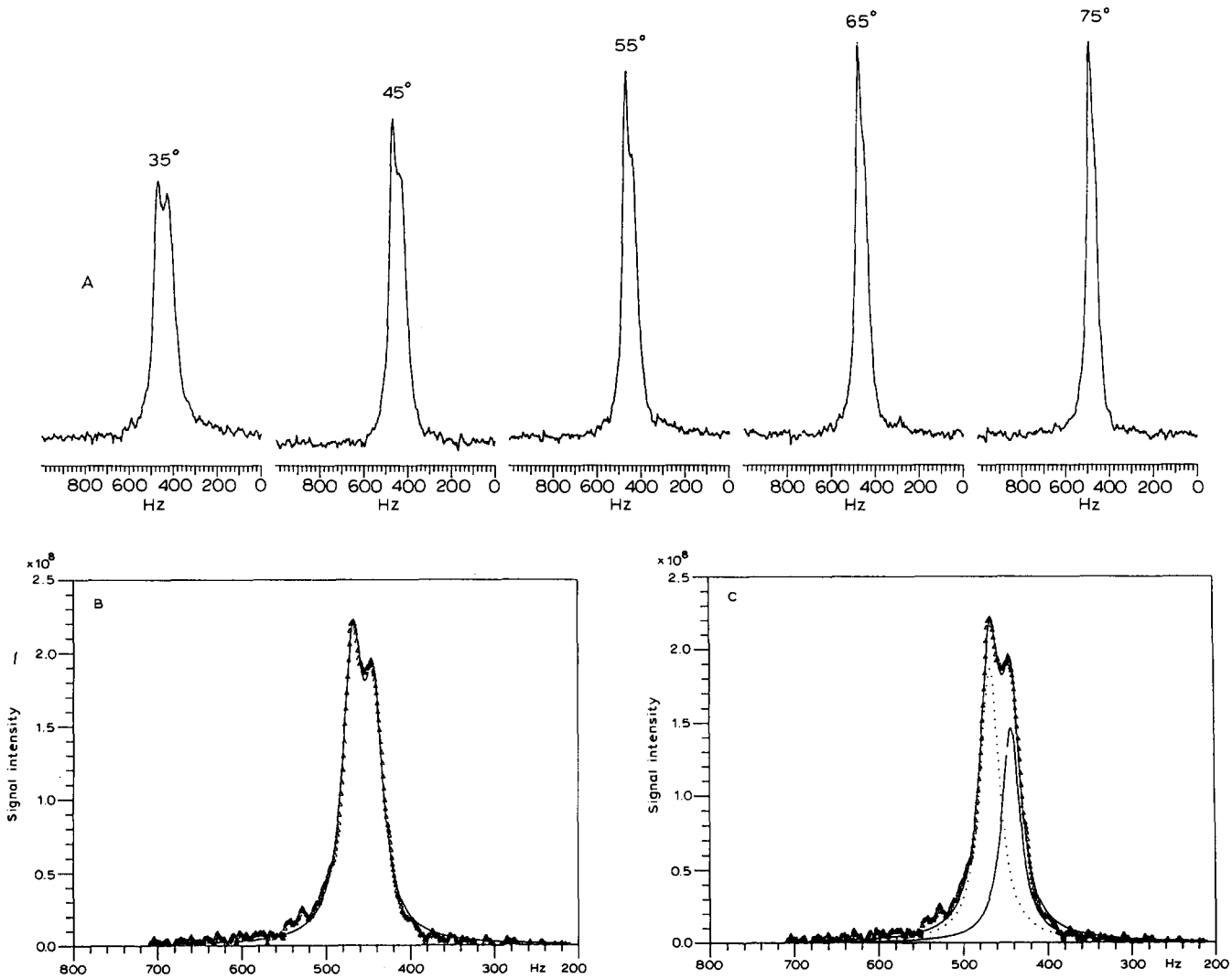

Fig. 5. (A) The temperature dependence of the proton-decoupled fluorine NMR spectrum at 376 MHz of the probe whose structure is shown in Fig. 1 bound to DMPC vesicles. Two thousand transients were averaged to obtain each spectrum. The lipid concentration was 10 mM in Hepes buffer and the probe-to-lipid mol% was 2. (B) An analysis of the spectrum obtained at 35 °C using the general line-shape function for two sites. The solid line is generated from the theoretical function, and the triangles are experimental points. Mean lifetimes (τ in Eqn. 5) on the order of 10^4 to 10^5 s must be assumed in order to fit the data over the temperature range indicated in part (A); the probe is thus not exchanging between the two classes of sites on the NMR time scale. The parameter values returned by the analysis of the indicated data are: $P_A = 0.41$, $T2_A = 122$ ms, $T2_B = 111$ ms, $\nu_A = 431.3$ Hz, $\nu_B = 466.4$ Hz, and $\tau = 1 \cdot 10^4$ s. (C) The fit of the probe fluorine NMR data shown as triangles to two overlapping Lorentzian line shape functions plotted as a solid line that is the sum of the individual lineshape functions also shown in the figure. The frequency scales shown in this figure are relative to the trifluoroacetic acid that was employed as an external reference; the single fluorine resonance from the reference is not shown in the spectra.

tenuated or essentially eliminated the lower frequency resonance present in the fluorine NMR spectrum obtained at 35 °C and shifted the resulting spectrum to higher frequencies. The shift caused by the spin label No. 522 was about 30 Hz (Fig. 4(B)) and was the largest observed for several spin labels (kit No. S-694) supplied by Molecular Probes, Inc. The fluorine spectrum from the probe bound to DMPC vesicles in the presence of spin label No. 556 at 5 mol% still contained a low frequency shoulder, and the maximum was shifted about 15 Hz to higher frequency. The effect of $Eu(FOD)_3$ on the spectrum was similar to that of spin label No. 522 in that the lower frequency resonance was apparently eliminated by this reagent, but the resulting spectrum was not shifted to any appreciable extent relative to that of the control. An analysis of the fluorine NMR spectrum area was performed by using trifluoroacetic acid as an external reference, in a coaxial capillary tube. In the presence of 1 mM $Eu(FOD)_3$, about 80 percent of the control spectrum area was still present. This analysis suggests that the primary effect of the former agent was to shift the lower frequency resonance into the higher frequency component to produce an apparently single resonance. Examination of the dye-DMPC vesicle system in the presence of $Eu(FOD)_3$ using electron microscopy, however, indicated that this shift reagent

tended to promote vesicle fusion in a manner similar to that caused by divalent cations such as Ca^{2+}. The 20 percent loss in area observed in the presence of this agent may be caused by spectral broadening due to the fusion process. The DMPC vesicle fusion process mediated by the probes diS-C_3-(5) and diS-C_4-(5) is known to result in a broadening of the DMPC ^{31}P resonance [28].

Vesicle fusion, however, could not be detected by electron microscopy when spin labels Nos. 522 and 556 were added to the DMPC preparation (Fig. 6). The presence of the two spin labels as well as $Eu(FOD)_3$ produce a pronounced reduction in the probe spin-spin relaxation time, T2, relative to that obtained from the dye fluorine NMR signal using control DMPC vesicles. This reduction in the relaxation time has been used to calculate the average distance of the CF_3 moiety from the paramagnetic site in the bilayer using the Solomon-Bloembergen relationship [40]

$$1/T2 = (4/60)S(S+1)[g_e^2\beta_e^2 g_N^2\beta_N^2/(\hbar^2 r^6)][7\tau_c + 13\tau_c/(1+\omega_s^2\tau_c^2)]$$
$$+(1/3)S(S+1)(a^2/\hbar^2)[\tau_e + \tau_e/(1+\omega_s^2\tau_e^2)] \quad (6)$$

where S is the intrinsic angular momentum of the electron, taken as $1/2\ \hbar$, g_N and g_e are the g factors for the fluorine nucleus and the electron, respectively, τ_c and τ_e are the correlation times characterizing the fluorine moiety tumbling rate and the unpaired electron effect on T2, respectively; ω_s is the angular resonance frequency of the electron in the 9.4 T magnetic field of the Varian VXR 400 spectrometer, and a is the coupling constant for coupling between the fluorine nucleus and the electron. Because of the restricted motion of the probe in the DMPC vesicle bilayer, the usual approximation of $\omega_s^2\tau_c^2 < 1$, which is valid for solutions, has not been made in the distance evaluations. The correlation time, τ_c, that appears in Eqn. 6 has been estimated using the molecular probe polarization and lifetime data obtained from vesicle-bound probe.

The T2 data used in the distance calculation were taken with the same DMPC preparation that was divided into a number of aliquots to which the individual spin labels previously identified were added. The effect of the spin labels on the T2 relaxation time was substantially larger than the effect of preparation aging over a three day period on this parameter. Relaxation time data are summarized in Table II.

The EPR spectrum of spin label No. 523 in the DMPC vesicles (Fig. 2) is qualitatively similar to the spectra reported for the same spin label in multilamellar lipid suspensions; a simple three line spectrum was observed. The order parameter describing the motion of the spin label/DMPC vesicle system, however, was consistently smaller than that describing the spin label motion in the multilamellar egg lecithin preparation. The latter difference is to be expected because of the vesicle tumbing effect; the spin label/DMPC vesicle system is thus well behaved. Accordingly, the location

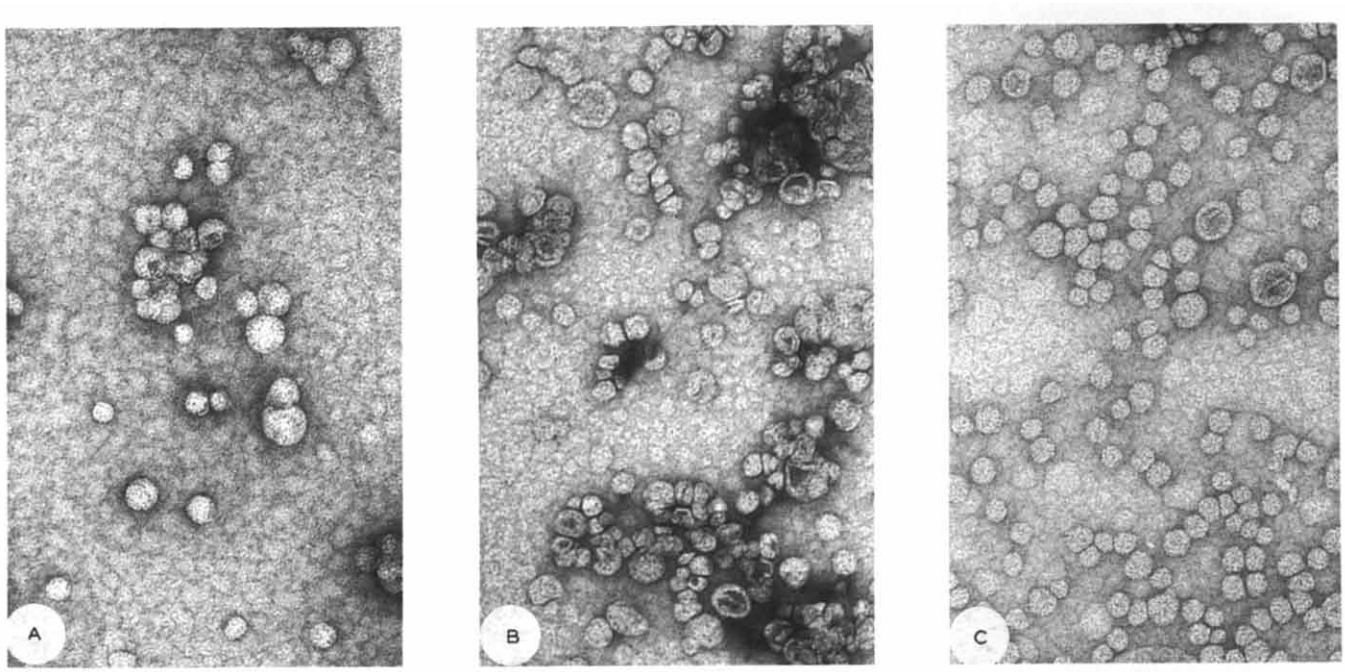

Fig. 6. Electron micrographs of dimyristoylphosphatidylcholine (DMPC) vesicles stained on a formvar grid with 1 percent uranyl acetate, obtained with a JEOL JEM-100CX II transmission electron microscope operating at 130000× magnification. Panel (A) contains a micrograph of the control sample, i.e., vesicles with no spin label present, whereas panels (B) and (C) contain micrographs of vesicles with spin labels Nos. 522 and 556 (Fig. 1) present at 5 mol%. These data indicate that the spin lables do not cause the DMPC vesicles to fuse or aggregate under the experimental conditions employed in the measurements described in this communication.

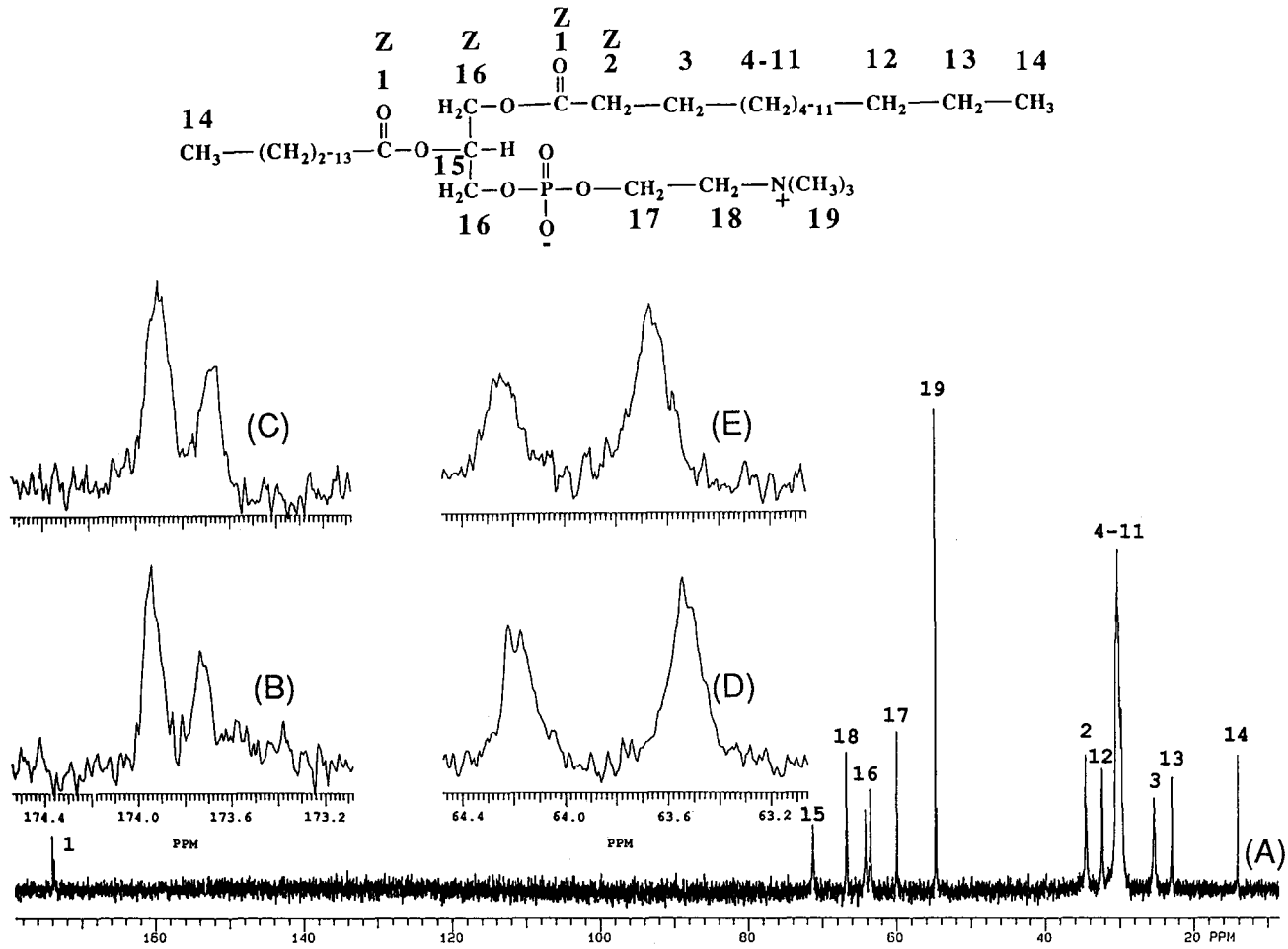

Fig. 7. (A) The ^{13}C spectrum of control DMPC vesicles at 10 mM in Hepes buffer. This spectrum, as well as those shown in insets (B) to (E), were obtained at 35 °C with complete proton decoupling using a Varian VXR 400 spectrometer operating at 100.6 MHz by averaging approx. 35000 transients with a line-broadening factor of 1 Hz. The resonance assignments are keyed to the lipid structure shown in the figure. The resonances from the groups labeled with the letter Z were broadened by 35 percent or more relative to the control by spin labels 522 and 556 (Fig. 1). The assignments of Birdsall et al. [43] for DMPC in solution were used as a guide in interpreting this and similar carbon spectra from the vesicles. In inset (C), the line-broadening and resonance-shifting effect of spin label 522 on the DMPC carbonyl resonances is illustrated at the same expansion in use for the control shown in inset (B). Inset (E) depicts these effects on the H_2C-O (No. 16) carbon resonance caused by spin label 556 relative to the control spectrum shown at the same expansion in part (D). The two spin labels were present at 2.5 mol%. The myristate terminal methyl group resonance was used as an internal reference and assigned a value of 14.1 ppm.

of the unpaired electron associated with the nitroxide group of the spin label was estimated from the effect of different spin labels on the lipid ^{13}C-NMR resonance line widths. Many of the resonances assigned to the control lipid spectrum (see Fig. 7(A)) were affected only marginally, but, for our purposes, we considered line broadening of 35 percent or more to be significant, and these effects were used in locating the trifluoromethyl group of the probe in the DMPC vesicles. The groups whose resonances were broadened as described are marked with the letter Z in Fig. 7.

Relative to the VXR 400 spectrometer transmitter frequency used for ^{13}C-NMR measurements, a constant reference for all ^{13}C DMPC NMR spectra, the chemical shift associated with the myristate terminal methyl resonance was invariant within ± 0.05 (S.D.) ppm in all DMPC vesicle preparations, including those containing the spin labels. Relative to tetramethylsilane (TMS), the lipid fatty acid terminal methyl resonance occurs at 14.1(± 0.1) ppm [41,42]. In our experiments, this resonance was unaffected by the spin labels, and it was used as in internal reference for the chemical shift scale shown in Fig. 7. The resonances broadened by 35 percent or more relative to the control DMPC ^{13}C spectrum were the carbonyl, the carbonyl methylene, and the H_2C-O moieties; the resonances corresponding to these groups are numbered 1, 2, and 16, respectively, in Fig. 7(A). The effect of spin labels No. 522 and 566 on the resonance linewidths and frequencies associated with the groups listed above are sumamrized in Table III. The effects of spin label No. 522 on the carbonyl resonance and of No. 556 on the H_2C-O resonance are shown in the insets labeled (C) and (E) in Fig. 7. The corresponding controls contained in parts (B) and (D),

TABLE III

Summary of the effect of lipophilic spin labels on the linewidths of ^{13}C-NMR resonances from DMPC unilamellar vesicles

Sample	Resonance frequency (Hz)	Linewidth at half-height (Hz)	Percent line-width increase	Resonance assignment
DMPC vesicle	6390.4	12.1	–	H_2C-O
control	6457.4	12.5	–	H_3C-O
Control +	6418.1	16.3 (17.1) *	26 (38) *	H_2C-O
2.5 mol%	6469.9	17.8	42.4	H_2C-O
spin label 522				
Control +	6468.6	17.7	46	H_2C-O
2.5 mol%	6409.3	19.0	52	H_2C-O
spin label 556				
DMPC vesicle	17472.9	7.0	–	C=O
control	17502.7	6.9	–	C=O
Control +	17476.9	12.1	73	C=O
2.5 mol%	17499.3	11.0	59	C=O
spin label 522				
Control +	17474.2	9.4	36	C=O
2.5 mol%	17496.6	9.4	35	C=O
spin label 556				
DMPC vesicle	3472.5	18.4	–	CH_2, No. 2
control	3477.9	9.6	–	CH_2, No. 2
Control +	3501.8	24.5	33 [a]	CH_2, No. 2
2.5 mol%	3501.8	24.5	155 [b]	CH_2, No. 2
spin label 522				
Control +	3497.5	21.1	15 [a]	CH_2, No. 2
2.5 mol%	3497.5	21.1	119 [b]	CH_2, No. 2
spin label 556				

[a] Line broadening was calculated using 18.4 Hz linewidth as the reference.
[b] Line broadening was calculated using 9.6 Hz linewidth as the reference.
* Line broadening was calculated using the algorithm supplied with the Varian VXR400 spectrometer software.

respectively, were obtained by expansion of the appropriate regions of the spectrum shown in Fig. 7(A). Linewidths at half-height were calculated using an algorithm provided in the Varian VXR 400 spectrometer software package as well as by hand. In the case of overlapping resonances, the half-linewidth at half-height was determined using the portion of the resonance that was the better resolved and the result multiplied by two. A considerable number of controls were carried out to investigate the reproducibility of the DMPC vesicle ^{13}C resonance linewidths. The reproducibility of the carbonyl, H_2C-O and methylene No. 2 resonance linewidths in different preparations with or without spin labels present fell in the 2 to 12 percent range, but occasionally was about 16 percent, depending on the specific resonance and the noise filtering procedure employed, i.e., by reducing zero filling or by the use of broadening factors or the absence thereof in the Fourier transformation of the IFD and subsequent correction of the linewidth for the broadening factor. Similar analyses were also performed for the terminal methyl group and methylene groups (Nos. 12 and 13 in Fig. 7). These groups are well removed from the apparent spin label unpaired electron locus and as expected were found to be unaffected by the presence of the spin labels. Linewidth increases caused by the spin labels are summarized in Table III and are well above the variation found in the controls.

Both DMPC vesicle-spin label preparations previously described were employed in the carbon NMR measurements. The effect of the unpaired electron on the carbon resonances was more localized in the premixed (chloroform solvent) preparations than in the case in which the label was added to preformed vesicles, but the same resonances were broadened by the factor of 35 percent or more in both types of preparations. The ^{13}C resonance assignments for DMPC in CD_3OD given by Birdsall et al. [43] were used as a guide in assigning the carbon spectrum from the DMPC vesicles (Fig. 7(A)).

Fluorescence spectroscopy

The emission spectrum of the free fluorinated molecular probe in the Hepes buffer, shown in Fig. 8, has a

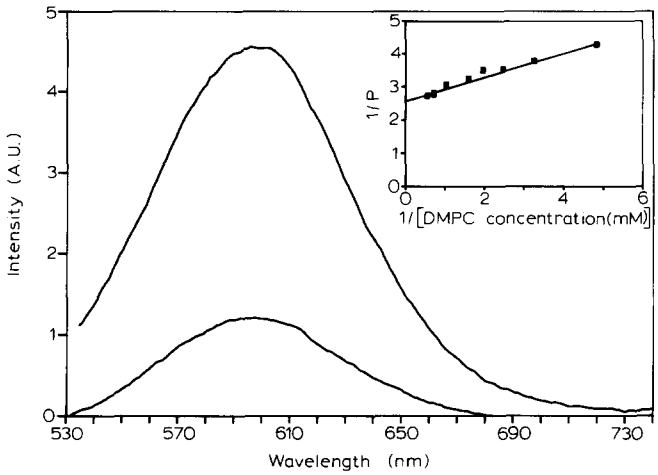

Fig. 8. The emission spectrum of the fluorinated probe in Hepes buffer. The lower trace is the emission spectrum of the free probe at 0.2 μM. The upper trace is the spectrum after addition of DMPC vesicles at 164 μM, 35°C, excitation wavelength = 525 nm, and slitwidths for ex = 6 nm and em = 2.5 nm. The inset contains a double-reciprocal plot of the degree of polarization, P, vs. the DMPC concentration and the linear regression line ($r^2 = 0.98$). The intercept on the ordinate corresponds to an infinite lipid concentration (all probe bound and $1/P = 2.57$). The initial probe concentration used in the titration with DMPC was 1.75 μM in Hepes buffer. The probe emission was monitored at 610.5 nm.

broad maximum near 600 nm. When an aliquot of DMPC vesicles was added to the probe solution, an increase in emission intensity was observed but no detectable shift in the maximum. The fluorescence lifetime of the free probe was shorter than 0.5 nsec, which is the limit of resolution for the method described, and hence was not measurable. The increase in quantum yield that apparently occurs when the probe was associated with the vesicles (Fig. 8) allowed the lifetime of the vesicle-bound probe to be measured. A double-exponential function was required in the nonlinear regression analyses, based on a Marquardt-Levenberg algorithm, to adequately describe the emission decay trace using the criterion that the reduced χ^2 is approximately unity. A typical decay curve is shown in Fig. 9. Lifetime values of 0.7 and 3 ns were obtained from these analyses. Approximately 90 percent of the decay curve amplitude, however, was associated with the shorter lifetime term in the double-exponential function.

The degree of polarization, P, characterizing the fluorinated probe fluorescence was calculated according to the relationship

$$P = [I_{\parallel} - I_{\perp}(I'_{\perp}/I'_{\parallel})]/[I_{\parallel} + I_{\perp}(I'_{\perp}/I'_{\parallel})] \quad (7)$$

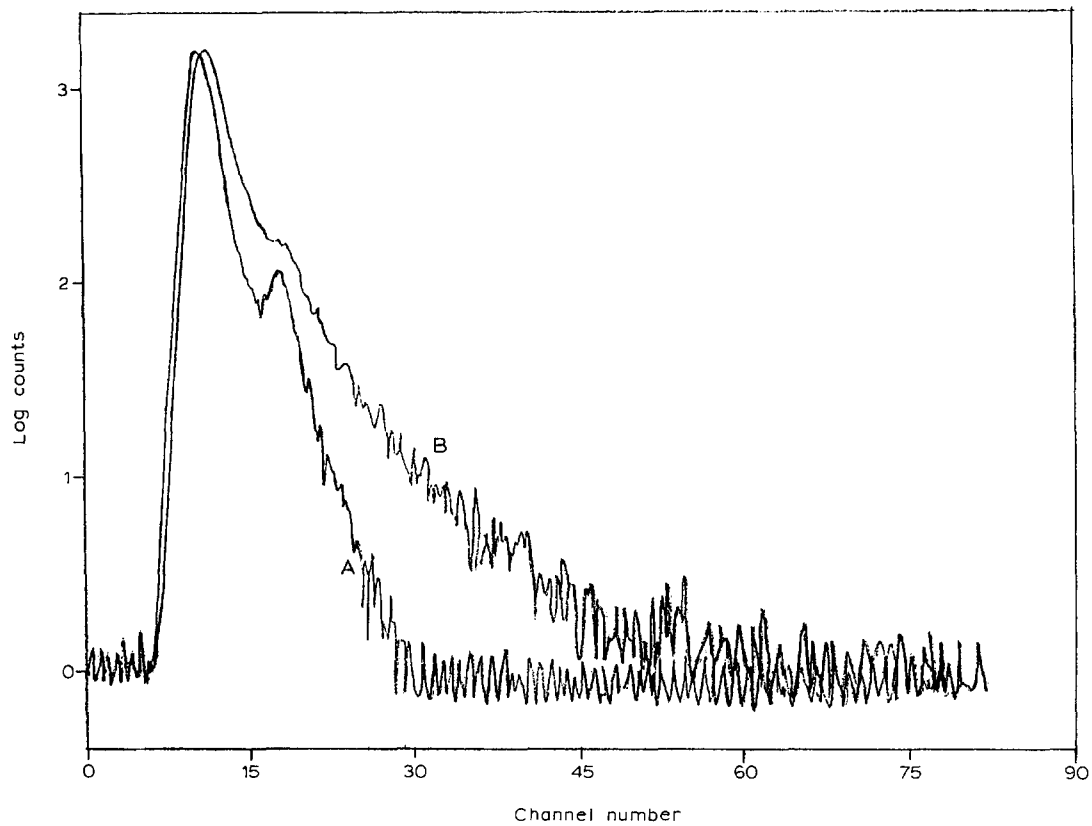

Fig. 9. Typical molecular probe fluorescence decay traces. Trace A is the instrument function characterizing the Photochemical Research Associates photon counting device at 525 nm; this trace was obtained using a scattering sample provided by the manufacturer. Trace B is that of the probe bound to DMPC vesicles suspended in Hepes buffer. The abscissa scale is provided in terms of bin numbers associated with the multichannel analyzer used in these measurements and is proportional to time. Approximately 10000 counts were averaged to obtain the decay curve shown in this figure. Probe lifetime values of 0.7 and 3 ns were obtained from analysis of the deconvoluted decay trace at 0.4 μM probe, 10 mM DMPC, and 35°C.

where $I_{\parallel}$ and $I_{\perp}$ are the intensities observed when the optic axes of the polarizers in the exciting and emitted light beams of the fluorometer are, respectively, parallel and perpendicular. The primed intensities are obtained by a 90 degree rotation of the polarizer positions relative to those associated with the unprimed intensities. The primed intensity ratio in parentheses is a correction for any pre-existing polarization in the fluorometer optics. This photoselection procedure for calculating P is discussed in detail by Azumi and McGlynn [44].

The combination of the degree of polarization with the corresponding lifetime (τ_F) allowed the determination of the fluorophore correlation time, τ_c, from the Perrin equation:

$$(1/P) - (1/3) = [(1/P_o) - (1/3)](1 + 3\tau_F/\tau_c) \quad (8)$$

In the preceding equation, P is the degree of polarization associated with the vesicle-bound fraction of probe and P_o is the limiting degree of polarization observed under conditions in which no fluorophore rotation occurs during the excited state lifetime. In general, the degree of polarization of the fluorescence from the probe in the presence of the DMPC vesicles will be a weighted average of the P values associated with the free and bound dye. In order to obtain the latter quantity, P was measured at fixed quantity of probe as a function of increasing DMPC vesicle concentration. A double-reciprocal analysis of the data involving a plot of $1/P$ vs. $1/$[DMPC] was linear; the intercept on the ordinate of the line obtained by a linear regression analysis of the data points obtained from the preceding titration was used in the Perrin equation (Eqn. 8). This intercept corresponds to the degree of polarization at infinite DMPC concentration, where all probe is bound. A typical plot is shown in the inset contained in Fig. 8.

In order to obtain P_o, associated with no fluorophore rotation during the excited state lifetime, fluorescence polarization measurements were performed on a solution of the dye in glycerol cooled to $-5\,^{\circ}$C. Cooled and dry nitrogen gas was used to purge the sample chamber to avoid water vapor condensation on the sample cuvette. The excitation and emission spectra characteristic of the probe in glycerol are shown in Fig. 10. Vibrational structure is discernible in the excitation spectrum. The solid and dashed lines plotted within each of these spectra are the degree of polarization as a function of probe excitation and emission wavelength, respectively. The degree of polarization was essentially independent of wavelength in both instances. Linear regression analyses of these data produced very low slopes and coefficients of determination (see the caption for Fig. 10). The average value of P over the excitation and emission wavelength ranges for which it could be determined was 0.47 to 0.48. These values are near the theoretical limit of 0.5 and indicate that the transition

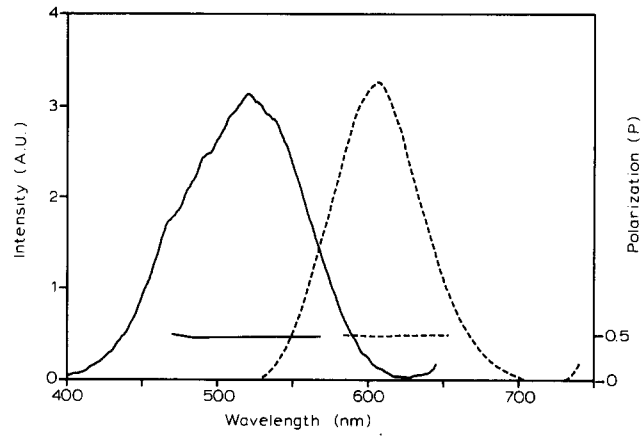

Fig. 10. The excitation (solid trace) and emission (dashed trace) spectra of the fluorinated probe (0.2 μM in glycerol at $-5\,^{\circ}$C). The solid line plotted with the excitation spectrum is the degree of polarization, P, as a function of the excitation wavelength, whereas the dashed line plotted with the emission spectrum is the degree of polarization as a function of emission wavelength. In both plots, P values were essentially independent of wavelength and approached the theoretical limit of 0.5. The slope of the solid line is $-4 \cdot 10^{-5}$ and $r^2 = 0.03$. The average value of P over the range of wavelengths covered by the solid line is 0.47 (± 0.009 (S.D.)). The slope of the dashed line is $-2 \cdot 10^{-5}$ and $r^2 = 0.04$. The average value of P over the wavelength interval corresponding to the dashed line is 0.48 (± 0.006 (S.D.)). The excitation spectrum was recorded using an emission wavelength of 650 nm and slitwidths of ex = 6 nm and em = 2.5 nm. The excitation wavelength used in obtaining the emission spectrum was 525 nm, and the slitwidths were ex = 3 nm and em = 2.5 nm. The polarization data obtained from these measurements were used for P_o in Eqn. 8 to obtain the probe rotational correlation time.

moments responsible for the excitation and emission spectra shown in Fig. 10 are nearly parallel. In subsequent determinations of the fluorescence P value for the molecular probe in the aqueous medium used for vesicle preparation at $35\,^{\circ}$C, a value of 0.49 was obtained, indicating that the free probe fluorescence lifetime is sufficiently short that no appreciable fluorophore rotation occurs during the excited-state lifetime, even when the medium viscosity is substantially less than that of chilled glycerol. The value of P determined from the double-reciprocal plot (inset in Fig. 8) and the value of P_o from the chilled glycerol solutions were used in the Perrin equation (Eqn. 8) to obtain a value of the correlation time τ_c. The degree of polarization values used in these calculations were those determined at 610.5 nm, but essentially the same values for these parameters were obtained at other wavelengths. Correlation times were calculated using both values of the fluorescence lifetime determined from the double-exponential analysis of the decay curve (Fig. 9); τ_c values are given in Table II and fall in the ns range. Calculation of the τ_c of a 300 Å diameter sphere in water at $35\,^{\circ}$C using Stokes' law yields a value of 2.4 μs and serves as an estimate of the τ_c for the DMPC vesicle global tumbling correlation time. The values in Table II

are approximately two orders of magnitude less than that obtained from Stokes' law, indicating that the vesicle-bound fluorinated probe has significant additional rotational freedom, i.e., the rotational relaxation of the bound dye is not governed exclusively by the vesicle tumbling rate.

Calorimetry

The calorimetrically determined enthalpy change, ΔH_{Cal}, and the cooperative unit parameter, CUP, characterizing the DMPC gel-to-liquid crystal phase transition are plotted as a function of mol percent probe in Figs. 11 and 12, respectively. The effect of the probe is to increase the enthalpy of the transition and to modestly decrease the temperature at the heat capacity profile maximum (T_m) as the mol percent value is increased. At 3.5 mol%, ΔH_{Cal} has increased by 27 percent relative to the control value, but T_m has monotonically diminished by only 2 percent. When the probe is present at 0.1 mol% or greater, the heat capacity profile becomes skewed on the lower temperature side; the profile obtained when the dye was present at 3.5 mol% could be readily deconvoluted into two components (Fig. 13). The latter observations suggest that multiple classes of probe sites are present in the DMPC preparation. The effect of the molecular probe on the

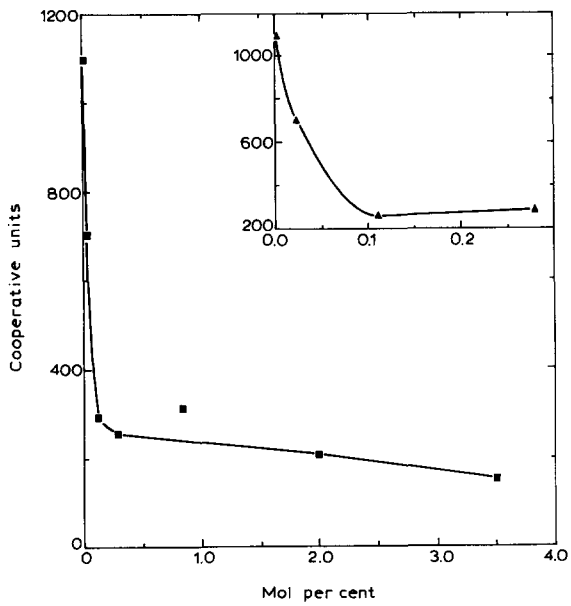

Fig. 11. Calorimetrically determined enthalpy changes, ΔH_{Cal}, for the gel-to-liquid crystal phase transition plotted vs. the mol percent of probe in the lipid phase (▲). The solid line was obtained from a linear regression analysis with the index of determination, $r^2 = 0.97$, an intercept = 5.58 kcal/mol, and slope = 368. Each point was derived from a determination, by numerical integration, of the area under the curve associated with plots like those shown in Fig. 13. The maxima of these curves (T_m) and the corresponding probe mol percentages are: 24.37°C, 0.000; 24.35°C, 0.022; 24.10°C, 0.11; 24.05°C, 0.28; 24.17°C, 0.84; 23.94°C, 2.2; and 23.85°C, 3.5.

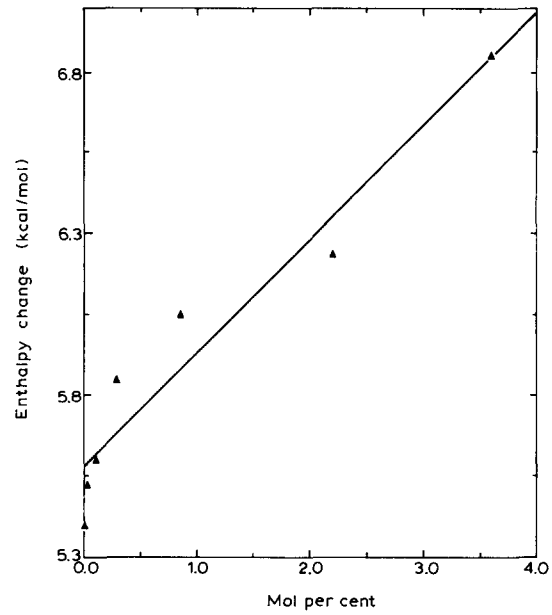

Fig. 12. Cooperative unit parameters for the DMPC gel-to-liquid crystal phase transition, defined as CUP = $\Delta H_{vH}/\Delta H_{Cal}$, plotted vs. the mol% of probe in the lipid phase. In the inset in the upper right, the region from zero to 0.3 mol% probe is shown on an expanded scale. Nearly 85 percent of the total effect of the probe on CUP occurs before 0.15 mol%.

cooperativity of the main DMPC transition is quite pronounced: when the probe is present at only 0.1 mol%, the CUP has decreased by 74 percent, but has decreased by 87 percent when it is present at 3.5 mol%. The marked decrease in the CUP but only modest changes in the ΔH_{Cal} and T_m values caused by the molecular probe suggest that it is behaving as a type A perturbant in the classification of Jain and Wu [45].

When the probe was present at 0.02 mol%, the behavior of the resulting system could be described by the ideal solution theory of Albon and Sturtevant [46] in which the probe is treated as an impurity; at higher mol% probe values, however, the behavior of the dye-DMPC system became markedly nonideal (see Fig. 13). The procedure for analyzing calorimetry data in terms of the ideal solution theory has been previously described in detail [47] and is only briefly described. The fraction of lipid, α, that has melted, i.e., exists in the liquid crystal form, is related to temperature T by

$$T/T_o = 1 - RT[(1/\Delta H_{vH}) \ln[(1-\alpha)/\alpha] + (\ln X_1/\Delta H_{Cal})[1/([K/(1-K)] + \alpha)]] \quad (9)$$

where T_o is the temperature at the midpoint of the phase transition for pure DMPC lipid in this case and X_1 is the mol fraction of lipid present. K is an equilibrium constant that describes the distribution of the

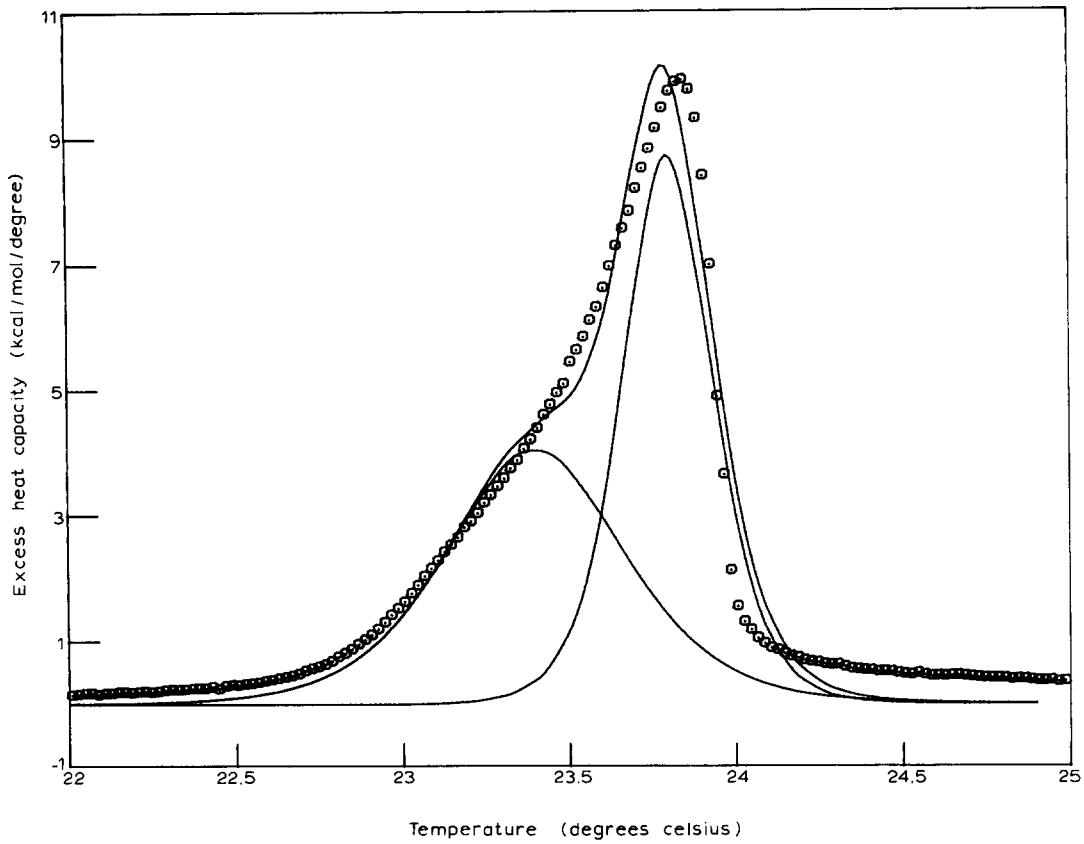

Fig. 13. The excess heat capacity in the region of the DMPC gel-to-liquid crystal phase transition with 3.6 mol% probe present. The transition region can be adequately represented by two overlapping two-state transitions: $T_1 = 23.4°C$, $\Delta H_1 = 2879$ cal/mol, and $CUP_1 = 344$; $T_2 = 23.8°C$, $\Delta H_2 = 3358$ cal/mol, $CUP_2 = 511$. The sum of these two transitions is the upper solid line which provides an adequate fit to the experimental data represented by circles (⊙).

impurity (molecular probe in this case) between the gel and liquid crystal phases and is defined by

$$K = X(\text{gel})/X(\text{liquid crystal}) \tag{10}$$

The remaining quantities that appear in Eqn. 9 have been previously defined. For a two-state model of the gel-to-liquid crystal transition, the excess heat capacity C_{ex} is given by

$$C_{ex} = (\Delta H_{Cal})(d\alpha/dT) \tag{11}$$

An expression for the derivative in Eqn. 11 was obtained from Eqn. 9 and substituted into Eqn. 11 to obtain

$$C_{ex} = [\Delta H_{Cal}\Delta H_{vH}/RT^2][1/\{(1/(1-\alpha)\alpha) - (\Delta H_{vH} \ln X_1/\Delta H_{Cal})(1/([K/(1-K)]+\alpha)^2)\}] \tag{12}$$

The fraction of melted lipid α that appears in Eqn. 12 was obtained at any temperature T by numerical solution of Eqn. 9 using the Newton-Rhapson method. The remaining parameters that appear in Eqn. 12 were either obtained by experiment or evaluated by fitting the calorimetry data to this equation using the nonlinear regression routine of Johnson and Schuster [39]. In carrying out the latter fitting procedure, ΔH_{Cal} and the mol fraction of lipid present in the probe-DMPC system, X_1, were considered to be known and held constant at the experimentally determined values. It was necessary in the initial analyses to select values of K and to hold these values constant during the fitting procedures; thus, the only floating variables were T_o and the van't Hoff enthalpy ΔH_{vH}. The following values of K were employed in the initial analyses: 10^2, 10, 10^{-1}, 10^{-2}, $5 \cdot 10^{-3}$, 10^{-3}, $5 \cdot 10^{-4}$, 10^{-6}, 10^{-8}, and zero. Values of the variance returned by the fitting routine and a comparison of the theoretical curve generated by substituting the parameters given by this routine into Eqn. 12 with the experimental data (see Fig. 14) indicated that satisfactory fits to the data were not obtained when K was greater than 10^{-2}. The variance became insensitive to the value of K when it was equal to or less than 10^{-3}. Subsequent analyses in which the values of ΔH_{vH}, T_o, and K obtained from the initial fitting procedures were used as initial estimates in the iteration procedure with K now being allowed to vary resulted in virtually the same values of these three parameters as the initial estimates being returned by the nonlinear regression routine. These results suggest that

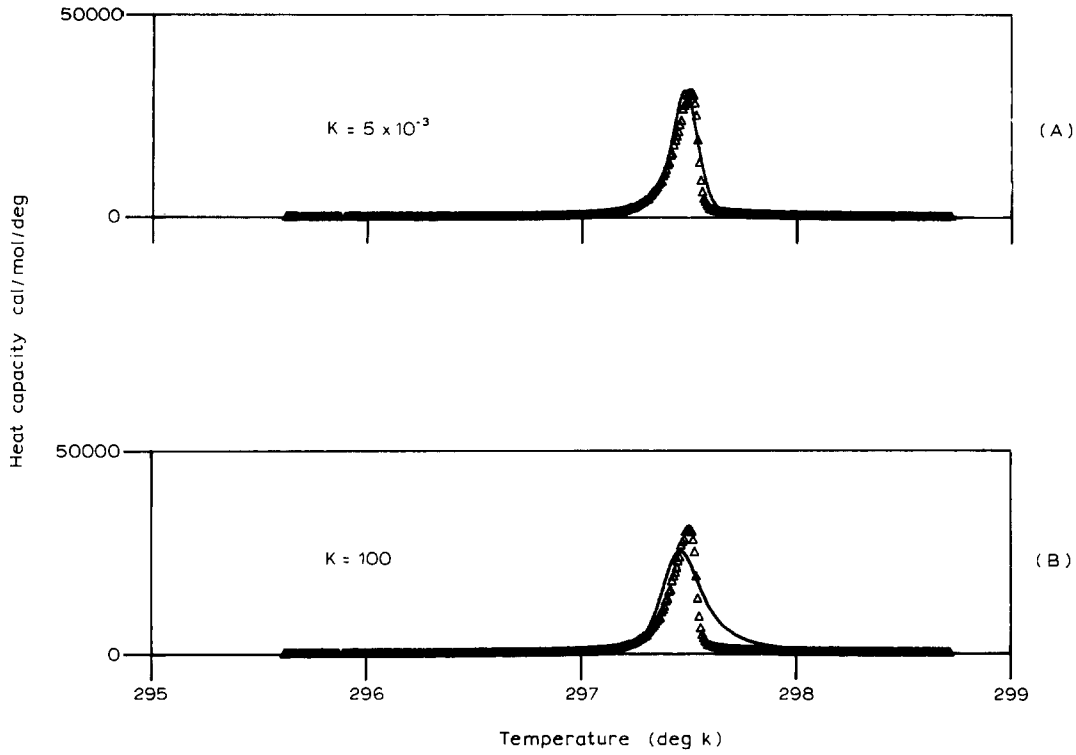

Fig. 14. Analyses based on the ideal solution theory of the excess heat capacity data describing the DMPC gel-to-liquid crystal phase transition when the fluorinated styryl probe was present at 0.02 mol%. In (A), the equilibrium constant K, defined by Eqn. 10, was $5 \cdot 10^{-3}$, and in (B) K was 10^2. The experimentally determined enthalpy change for the transition and the mol fraction of lipid were held constant at $\Delta H_{Cal} = 5525$ cal/mol and $X_1 = 0.9998$, respectively. This analysis yielded values of the van't Hoff enthalpy change, ΔH_{vH}, and the temperature at the midpoint of the transition for pure DMPC lipid, T_o, of $4.6 \cdot 10^6$ cal/mol and 297.48 K, respectively. The corresponding experimentally determined values were: $3.9 \cdot 10^6$ cal/mol and 297.5 K, respectively.

the behavior of the probe-DMPC system when the probe is present at very low mol percentages is not sensitive to the value of K provided that it is equal to or less than 10^{-2} to 10^{-3}. Typical fits to the experimental excess heat capacity profile using the preceding analyses are shown in Fig. 14 with $5 \cdot 10^{-3}$ and 10^2 values for K; clearly the former value leads to a satisfactory description of the data and the latter value does not.

It has been previously shown [47] that the enthalpy change, ΔH_{TRANS}, associated with the transfer of the probe from the gel to the liquid crystal phase, is given by

$$\Delta H_{Cal} = \Delta H^0 + [(1 - X_1)/X_1]\Delta H_{TRANS} \quad (13)$$

where ΔH^0 is the enthalpy change for the gel-to-liquid crystal phase transition of the control DMPC multilamellar preparation. ΔH_{TRANS} was obtained by a linear regression analysis of a plot of ΔH_{Cal} vs. $(1 - X_1)/X_1$ (Fig. 11). The equilibrium constant describing this process, $K^{-1} = 10^2$, obtained from the preceding ideal solution analyses, was combined with ΔH_{TRANS} in standard thermodynamic relationships to yield the corresponding entropy change, ΔS_{TRANS}. The value of K obtained from the ideal solution theory analyses, 10^{-2} to 10^{-3}, indicates that the probe distribution favors the liquid crystal phase; however, values for ΔH_{TRANS} and ΔS_{TRANS} obtained from these calculations were 36.8 kcal/mol and 133 cal/mol per K, respectively. The positive values obtained for these parameters indicate that the dye is strongly associated with the DMPC lipid in the gel phase and that this association is reduced in the liquid crystal phase. This unfavorable effect, however, is overcome by the pronounced increase in entropy that the probe acquires in the liquid crystal phase, i.e., the dye has substantially increased mobility, as expected from the known fluidity of this phase. The transfer process is thus entropically driven. The positive ΔH_{TRANS} value is also consistent with the pronounced reduction in the CUP caused by the probe; the strong association of this probe with DMPC in the gel phase would tend to reduce the lipid–lipid interactions necessary for high cooperativity of the gel-to-liquid crystal phase transition. In previous work on probes with similar structures [47], the K^{-1} for transfer was near 2 and ΔH was either near zero or in the -15 to -45 kcal/mol range. This probe thus interacts much more strongly with DMPC in the gel phase than do previously-studied probes of similar structure; such interaction favors an orientation in which the long axis of the probe is parallel to the hydrocarbon chains. The positive charge must be near the phosphate group that bears a negative

charge, and the remainder of the probe could be buried in the hydrocarbon region. In such a complex, the methylene groups on the hydrocarbon chains of the probe would make contact with the methylenes on the lipid fatty acid chains. The order of such a complex would be reduced in the liquid crystal phase; thus both ΔH_{TRANS} and ΔS_{TRANS} are predicted to be positive, as observed. The negative sign for ΔH_{TRANS} found in previous work with other probes may indicate that these probes are located in the hydrocarbon region of the bilayer only in the liquid crystal phase.

Molecular mechanics calculations

A model based on the distances from the site of the unpaired electron associated with the lipophilic spin label to the locus of the fluorinated molecular probe has been generated using the molecular mechanics package MACROMODEL executing on a Microvax II Q5 computer. Before the actual probe-lipid complex inferred from the results described in the preceding sections was assembled, the energies of an isolated all-*trans* DMPC and a probe molecule were minimized using the Amber and the MM-2 force field parameters, respectively. The

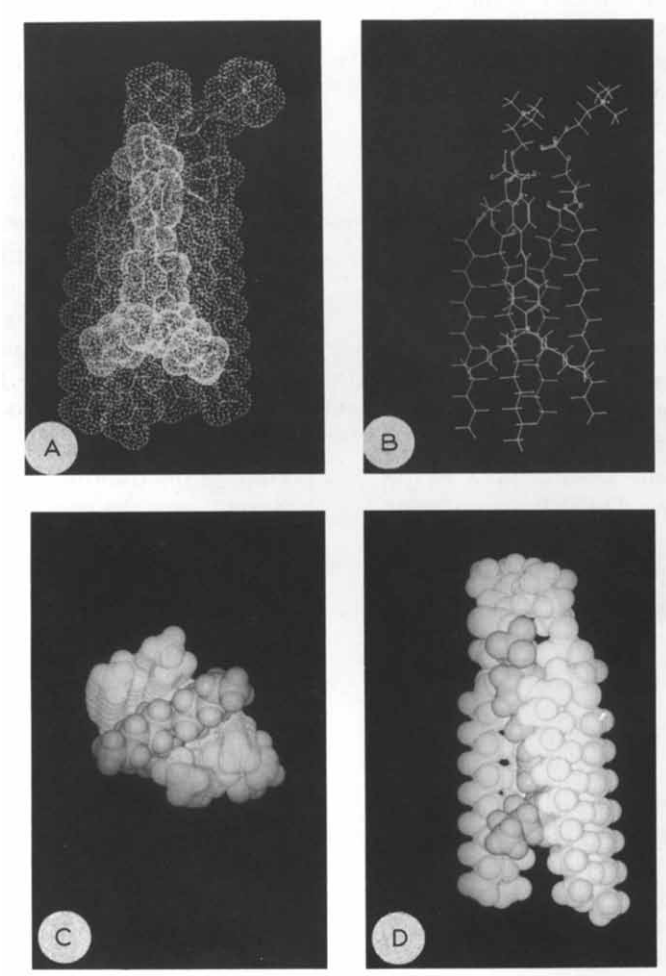

Fig. 15. A probe location model derived from a knowledge of the spin label locus in the bilayer and the distance from the latter site to the probe fluorine moiety. Because this distance was projected along the bilayer normal, the styryl probe location corresponds to the minimum probe penetration into the model membrane compatible with the experimental results. In panel (A), the probe is shown intercalated between two DMPC lipids with spheres derived from the van der Waal's radii. The styryl probe is illustrated at higher density than that of the lipids. Panel (B) illustrates the same complex but without the spheres. Panel (C) contains a bottom view of the complex in a CPK model format. Panel (D) is a side view of the complex in a CPK rendering. The structure of the preceding probe-DMPC complex was optimized by energy minimization using the molecular mechanics package MACROMODEL. In these calculations, the energies of the probe and a DMPC molecule were separately minimized using the MM-2 and AMBER force field parameters, respectively. The complex shown in this figure was then assembled using the docking facility of the package and the energy of the complex minimized. The initial choice of locating the ring structures and *n*-pentyl groups of the styryl probe in the hydrocarbon region of the bilayer was based on energy considerations and the sensitivity of the DMPC gel-to-liquid crystal phase transition cooperativity to the presence of this probe (Fig. 12). Calculations based on both the MM2 and AMBER force fields were carried out with distance-dependent dielectric constants. A multiplier value of unity was employed for the illustrated structures. Additional calculations on the probe/DMPC complex were carried out with a multiplier of 4. The higher dielectric constant resulted in less repulsion between the choline headgroups which were positioned closer together than in the complex illustrated in this figure; the remainder of the complex structure, however, was essentially unaltered.

trans form of the dye was predicted to be more stable than the *cis* conformation by approx. 300 kJ/mol and was used in assembling the probe-lipid model. In order to generate an initial trial probe-lipid complex, the molecular docking feature of MACROMODEL was used to assemble one DMPC and one dye molecule at sufficiently close proximity that contact between the probe and lipid van der Waals radii occurred. In this assembly procedure, the distance from the spin label site to the fluorine-containing moiety was projected along the lipid long axis and the trifluoromethyl group of the probe sited at the resulting location. This probe-DMPC lipid assembly procedure was carried out at high resolution using an Evans and Sutherland model 390 molecular graphics system supported by the Microvax II computer. The necessary trigonometric calculations for determining the probe trifluoromethyl group site are readily performed by the MACROMODEL package. The distance obtained using the spin label No. 556 was somewhat larger than that resulting from No. 522 (Table II), but the unpaired electron associated with it was located at a site somewhat deeper into the hydrocarbon region of the bilayer than was that of No. 522. Thus, essentially the same location for the fluorinated probe in the bilayer was obtained from the effects of both spin labels on the fluorine T2 relaxation time. The energy of this complex was then minimized using the AMBER force field constants. A second DMPC lipid in the conformation resulting from the AMBER energy minimization was then added to this complex using the docking procedure. The resulting assembly was again subjected to energy minimization using AMBER force field constants. The resulting model is shown in Fig. 15(A)–(D).

Discussion

The use of fluorine NMR in the preceding investigations allows a signal unique to the molecular probe to be readily detected without the attendant severe background problems that would be associated with the use of proton NMR spectroscopy to locate the probe in the DMPC bilayer. Additional advantages of this approach are that the fluorine nucleus is 100 percent abundant, has a spin of one-half (no quadrupole moment), has a wide chemical shift range, and has about 90 percent of the sensitivity of the proton based on a comparison of the ratio of the gyromagnetic ratio to the percent abundance of the two nuclei.

A number of assumptions, however, have been made in evaluating the distance from the spin label site to that of the trifluoromethyl moiety. Implicit in the use of the fluorophore rotational correlation time obtained from the Perrin equation (Eqn. 8) in Eqn. 6 to determine this distance is that the motion of the membrane-bound fluorinated probe is reflected by the correlation time, and that internal motion within the probe is restricted. However, when the molecular probe is bound to vesicles at high lipid-to-probe mol ratios, the fluorine resonances are broadened substantially, indicating that the trifluoromethyl group is located some distance from the surface of the bilayer, and that motion of this group is highly restricted. The small fluorescence lifetime of the probe bound to the vesicles (Table II) implies that relatively little molecular motion occurs during the time period over which the first excited singlet state is occupied and, as indicated by the form of Eqn. 8, tends to favor diminished values for the correlation time. The value of the degree of polarization (0.49), near the theoretical limit observed even for the probe in Hepes buffer at 35 °C also is in agreement with this conclusion. The distance obtained from Eqn. 6 varies as the sixth root of the correlation time, thus is not highly sensitive to changes in the value of the former parameter. Similar distance values were obtained, for example, from the T2 relaxation time reduction caused by the spin labels when either of the two correlation times corresponding to the two fluorescence lifetime values obtained from the double exponential analysis were used in Eqn. 6 (see Table II).

The second term in Eqn. 6 is due to a contact interaction requiring that unpaired electron density be present at the fluorine nuclei in the system under investigation. Since the spin label with the unpaired electron localized primarily in the N-O group and fluorinated probe are separate molecular entities with no covalent bonding between them, and these moieties are likely some distance apart in the bilayer, the probability of the required overlap of the wavefunctions from the two molecules occurring to an extent sufficient to lead to a significant contribution from the contact term to the relaxation rate processes characterizing the probe T2 value is considered to be small; therefore, the latter term has been neglected in the distance evaluation. This calculational procedure is equivalent to the assumption that the contribution of the unpaired electron to the relaxation rates characterizing $T1^{-1}$ and $T2^{-1}$ is the same, provided that the experimental conditions are such that $\omega_s^2\tau_c^2 \ll 1$. The latter constraint is not necessarily met in the probe-DMPC vesicle system, due to restricted motion of the probe molecule in the bilayer. The latter restriction on probe motion, however, is unlikely to be operative when the probe is dissolved in CD_3OD; the fluorine T1 and T2 values obtained from such a sample, while not identical, are quite similar; furthermore, the effect of $Eu(FOD)_3$ on the $T1^{-1}$ and $T2^{-1}$ values is likewise similar. (The spin labels were not used in this test because of their low solubility in methanol.) For example, the changes in the preceding two parameters on peak No. 2, Table I, caused by the presence of 1 mM shift reagent are 0.32 and 0.58 s^{-1},

respectively. The use of these values in Eqn. 3 with the second term neglected would lead to distances that differ by only 10 percent. Furthermore, the average distance of approach of the probe and shift reagent in solution is likely much closer than that possible between the probe and the spin label in the DMPC bilayer, and so the contribution of the contact term in Eqn. 3 would likely be more pronounced on the relaxation rates of the probe in solution than when it is bound to the DMPC vesicles. These results, as well as the earlier conclusions suggest that the error introduced by the neglect of the contact term in the distance calculations is not significant in relation to that from other assumptions inherent in this procedure.

The distance evaluation previously described provides an estimate of the relative location of the spin label and the probe trifluoromethyl moiety but does not directly relate to the positioning of the remainder of the probe molecule within the bilayer. The probe is asymmetrical, one end is positively charged, whereas hydrophobic *n*-pentyl groups are bound to the other side of the ring system (Fig. 1). In order to achieve minimal energy, the hydrophobic portion of the probe molecule is expected to occupy a position in the hydrocarbon portion of the bilayer, as shown in the proposed model obtained from the molecular mechanics calculations (Fig. 15). Here, the pentyl groups have been positioned to cause minimal separation of the originally adjacent lipids as the probe intercalates between the two lipid hydrocarbon regions. The long axes of the probe and lipid need not be exactly parallel in the vesicle bilayer, but lipid packing forces acting on the probe in the bilayer would tend to favor an approximately parallel orientation.

Even when present at only 0.02 mol%, the fluorinated styryl molecular probe causes a marked decrease in the cooperativity of the DMPC gel-to-liquid crystal phase transition, essentially nullifying the cooperativity when present at 0.3 mol%. This marked reduction in the phase transition cooperativity suggests that this asymmetrical probe penetrates deeply into the hydrocarbon region of the DMPC bilayer and tends to diminish interactions between neighboring lipid fatty acid chains, a finding consistent with the model illustrated in Fig. 15. Similar asymmetrical probes, such as the styryl indicator RH 160 and merocyanine 540 (M540), cause similar marked reductions in the DMPC gel-to-liquid crystal phase transition when present at low mol percent, an observation that suggests that these probes also penetrate deeply into the bilayer with the long axes approximately parallel to the bilayer normal, at least when the bilayer is in the liquid crystal phase [47]. In contrast, the surface-active, symmetrical probe diS-C_3-(5) has only a minimal effect on the cooperativity parameter, and remarkably, the excess heat capacity data for the main DMPC phase transition in the presence of diS-C_3-(5) at 11 mol% can still be described by ideal solution theory [47].

Furthermore, Loew et al. [48] have shown that the electrochromic indicator di-5-ASP, whose structure is similar to that of the fluorinated probe shown in Fig. 1, exhibits a marked tendency to orient in hemispherical bilayers so that the long axis of the probe is approximately parallel to the bilayer normal.

The large and positive value of ΔS_{TRANS} indicates that the fluorinated molecular probe acquires substantial mobility in the DMPC liquid crystal phase, in which the NMR measurements were performed and for which a location model was developed. Substantial displacement of the probe can occur, however, via lateral diffusion that involves either transient association of the probe with successive lipids or concerted lateral motion of the probe and several tightly associated DMPC molecules without affecting the depth of the probe penetration into the bilayer.

The distance values obtained have been projected along the long axis of the lipids, i.e., along the bilayer normal. The resulting position of the probe thus corresponds to the minimum penetration of the dye into the bilayer that is consistent with the spin label to fluorine moiety distance values. Since spin labels located off the long axis would also likely contribute to the T2 reduction process, the average probe position may be associated with a slightly deeper probe penetration into the bilayer than that shown in Fig. 15.

Even for the case of minimal probe penetration, the upper end of the optical chromophore, consisting of the two ring systems and the two-carbon conjugated chain connecting them, is located near the carbonyl groups of the fatty acids; the chromophore extends into the hydrocarbon region from this point. This model thus predicts that the probe optical chromphore is probably sufficiently far from the membrane surface/headgroup region to render it relatively insensitive to changes in ionic strength and associated surface charge density alterations [20] or those associated with ion translocation [22,23].

The fluorine NMR spectrum of the molecular probe bound to DMPC vesicles consistently exhibited two partially resolved resonances with approximately equal populations (Figs. 4 and 5), an observation that suggests that the probe occupies two distinct classes of sites. The effect of a number of lipophilic spin-labels as well as $Eu(FOD)_3$ on the spectrum appeared to be largely confined to the lower frequency component of the NMR spectrum. Since both shift reagent and the spin labels were added to a probe-DMPC preparation, each is expected to localize first in the outer leaflet of the bilayer but to eventually translocate to the inner leaflet. The latter translocation process in this preparation, however, is likely to be slow, as judged from the observation that after the addition of $Eu(FOD)_3$, the

DMPC vesicle ^{31}P-NMR signal remained essentially invariant over a 24 h period. The two resonances may thus correspond to probe sites in the inner and outer leaflets of the unilamellar vesicles. Heating the probe-DMPC vesicle system tended to collapse the splitting between the two resonances suggesting that as the temperature is increased, the two sites become magnetically equivalent possibly due to enhanced mobility of the fluorinated probe in the two classes of sites.

A model in which two classes of probe sites are present in both bilayer leaflets but at different depths from the surface cannot be eliminated, but in one of these two types of sites the trifluoromethyl group would be required to be some 20 Å from the spin label site, since at the latter distance, the effect of the spin label on the probe ^{19}F relation time is not distinguishable from the 4 percent error in the evaluation of the control relation time, and because one of the fluorine resonances appears to be only marginally affected by paramagnetic perturbants. This distance requirement would place a considerable portion of the molecular probe in contact with either the bulk aqueous medium at the surface of the bilayer or the medium known to be present in the lipid headgroup/glycerol backbone interface region. A portion of the hydrophobic region of the probe would also likely be in contact with the aqueous phase, a location that is at least entropically unfavorable, since water molecules would be required to solvate the exposed probe region.

Two lifetimes were extracted from the fluorescence decay curve of the probe bound to DMPC vesicles. In contrast to the nearly equal populations associated with the fluorinated probe NMR resonances, approximately 90 percent of the decay curve amplitude was associated with the shorter-lived probe species. This difference in amplitude, however, may reflect differences in the quantum yield of the probe species occupying the two classes of sites possibly linked to known differences in lipid packing density associated with the two bilayer leaflets. The possibility that one of the observed fluorescence lifetimes is due to free probe can be eliminated, since the lifetime of the free probe was too short to be measurable by the apparatus employed in these investigations.

When the styryl probe was present in multilamellar DMPC preparations used in the calorimetry measurements at mol percentages near those employed in the fluorine NMR and fluorescence lifetime measurements, at least two transitions with approximately equal ΔH values were required to fit the heat capacity data (see Fig. 13). The existence of multiple classes of probe sites in the vortexed DMPC preparation is thus also apparent, but whether these sites are the same as those detected by the NMR and optical spectroscopy work cannot be determined from the available data.

It has also been possible to readily obtain the fluorine NMR spectrum from the probe shown in Fig. 1 bound to bovine heart submitochondrial particles. The techniques employed in the DMPC vesicle work may thus also be usable in functional membrane preparations for developing probe location models in these systems.

Acknowledgments

These investigations were supported by NIH award GM30552 and by equipment awards 2-4-01008 and CHE8409599 from the Department of Education and NSF, respectively. The authors have greatly benefited from the assistance of Dr. R.W. Jones, Dr. S. Woehler, and Mr. D. Harden in the performance of the molecular mechanics calculations. The authors also thank Professor W. Nelson for assistance in recording EPR spectra, Professor Isiah Warner for the use of his fluorescence lifetime apparatus, Dr. G. Nelson for assistance in the initial measurements, and Mr. R. Simmons for assistance in electron microscopy procedures.

References

1 Waggoner, A.S. (1976) J. Membr. Biol. 27, 317.
2 Waggoner, A.S. (1979) Annu. Rev. Biophys. Bioeng. 8, 47–68.
3 Waggoner, A.S. and Grinvald, A. (1977) Ann. N.Y. Acad. Sci. 303, 217–241.
4 Bashford, C.L. and Smith, J.C. (1979) Meth. Enzymol. 55, 596.
5 Bashford, C.L. (1981) Biosci. Rep. 1, 183.
6 Smith, J.C. (1988) in Spectroscopic Membrane Probes (Loew, L.M., ed.), Vol. 2, pp. 153–197, CRC Press, Boca Raton, FL.
7 Cohen, L.B. and Salzberg, B.M. (1978) Rev. Physiol. Biochem. Pharmacol. 83, 35.
8 Cohen, L.B., Salzberg, B.M., Davila, H.V., Ross, W.N., Landowne, D., Waggoner, A.S. and Wang, C.H. (1977) J. Membr. Biol. 19, 1–36.
9 Ross, W.N., Salzberg, B.M., Cohen, L.B., Grinvald, A., Davila, H.V., Waggoner, A.S. and Wang, C.H. (1977) J. Membr. Biol. 33, 141–183.
10 Optical Methods in Cell Physiology (1986) (De Weer, P. and Salzberg, B.M., eds.), Wiley Interscience, New York.
11 Spectroscopic Membrane Probes (1988) (Loew, L.M., ed.), CRC Press, Boca Raton, FL.
12 Williams, R.J.P. (1961) J. Theor. Biol. 1, 1.
13 Chance, B. (1977) Annu. Rev. Biochem. 15, 1941.
14 Malpress, F.H. (1984) J. Theor. Biol. 109, 501.
15 Kell, D.B. (1979) Biochim. Biophys. Acta 549, 55.
16 Slater, E.C., Berden, J.P. and Herweijer, M.A. (1985) Biochim. Biophys. Acta 811, 217.
17 Ferguson, S.J., Lloyd, W.J. and Radda, G.K. (1976) Biochim. Biophys. Acta 423, 174.
18 Haynes, D.H. (1974) J. Membr. Biol. 17, 341.
19 Chiu, V.C.K., Mouring, D., Watson, B.D. and Haynes, D.H. (1980) J. Membr. Biol. 56, 121.
20 Kinally, K.W., Tedeshi, H. and Maloff, B.L. (1979) Biochemistry 17, 3419.
21 Laris, P.C., Bahr, D.P. and Chaffee, R.R.J. (1975) Biochim. Biophys. Acta 376, 415–425.
22 Beeler, T.J., Farmen, R.H. and Martonosi, A.N. (1981) J. Membr. Biol. 62, 113.

23 Russell, J.T., Beeler, T.J. and Martonosi, A.N. (1979) J. Biol. Chem. 254, 2040.
24 Ehrenberg, B., Meiri, Z. and Loew, L.M. (1984) Photochem. Photobiol. 39, 199.
25 Orbach, H.S., Cohen, L.B. and Grinvald, A. (1985) J. Neurosci. 5, 1886–1895.
26 Blasdel, G.G. and Salama, G. (1986) Nature (London) 321, 579–585.
27 Suurkuusk, J., Lenz, B.R., Barenholz, Y., Biltonen, R.L. and Thompson, T.E. (1976) Biochemistry 15, 1393.
28 Bammel, B.P., Brand, J.A., Simmons, R.B., Evans, D. and Smith, J.C. (1987) Biochim. Biophys. Acta 896, 136–152.
29 Heinonen, J.R. and Lahti, R.J. (1981) Anal. Biochem. 113, 313–317.
30 Gordon, L.M. and Sauerheber, R.D. (1977) Biochim. Biophys. Acta 466, 34–43.
31 Seelig, J. (1970) J. Am. Chem. Soc. 92, 3881–3887.
32 Hubbell, W. and McConnell, H.M. (1971) J. Am. Chem. Soc. 93, 314–326.
33 Privalov, P.L. (1980) in Biological Microcalorimetry (Beezer, T., Ed.), pp. 413–453, Academic Press, New York.
34 Biltonen, R.L. and Freire, E. (1978) CRC Crit. Rev. Biochem. 5, 85–124.
35 Thompson, L.K., Sturtevant, J.M. and Brudvig, G.W. (1986) Biochemistry 25, 6161–6169.
36 Zimm, B.H. and Bragg, J.K. (1959) J. Chem. Phys. 31, 526–535.
37 Kanehisa, M.I. and Tsong, T.Y. (1978) J. Am. Chem. Soc. 100, 424–432.
38 Martin, M.L., Martin, G.J. and Delpuech, J.-J. (1980) Practical NMR Spectroscopy, pp. 295–297, John Wiley and Sons, Ltd., London.
39 Johnson, M.L. and Schuster, T.M. (1974) Biophys. Chem. 2, 32–41.
40 Carrington, A. and McLachlan, A.D. (1967) Introduction to Magnetic Resonance, p. 228, Harper and Row, New York.
41 Hamilton, J.A. and Small, D.M. (1981) Proc. Natl. Acad. Sci. USA 78, 6878–6882.
42 Spooner, P.J.R., Hamilton, J.A., Gantz, D.L. and Small, D.M. (1986) Biochim. Biophys. Acta 860, 345–353.
43 Birdsall, N.J.M., Feeney, J., Lee, A.G., Levine, Y.K. and Metcalfe, J.C. (1972) Chem. Soc. (London), Perkin Trans. II, 10, 1441–1445.
44 Azumi, T. and McGlynn, S.P. (1962) J. Chem. Phys. 37, 2413.
45 Jain, M.K. and Wu, N.M. (1977) J. Membr. Biol. 34, 157–201.
46 Albon, N. and Sturtevant, J.M. (1978) Proc. Natl. Acad. Sci. USA 75, 2258–2260.
47 Fumero, J., Bammel, B.P., Hopkins, H.P. and Smith, J.C. (1988) Biochim. Biophys. Acta 944, 164–176.
48 Loew, L.M., Scully, S., Simpson, L. and Waggoner, A.S. (1979) Nature 281, 497.